COMPOSITION OF THE UNIVERSE

In the case that ***lower-energy hydrogen, hydrinos, comprises the dark matter***, all matter is ordinary (baryonic) matter, and the mass of the Universe is sufficient for it to be closed [30, 31]. Whereas, the standard theory of big bang nucleosynthesis explains the observed abundance of light elements (H, He, and Li) only if the present density of ordinary (baryonic) matter is less than 10 % of the critical value [43, 44]. Recently, the missing mass has been showed to be baryonic rather than strange matter [45]. According to classical physics (CP), ***the abundance of the lighter elements, H, He, and Li can be explained by neutron, proton, and electron production during the contraction phase and stellar nucleosynthesis during the contraction as well as the expansion phase of the expansion-contraction cycle***. In the latter case, stellar and galaxy evolution occurred during the contraction phase as revealed by high-redshift radio galaxies and galaxies associated with extremely distant, luminous quasars that date back to the beginning of the expansion [46, 47]. The presence of metal lines in quasars demand a previous generation of stars (two generations for nitrogen) that is consistent with the stellar nucleosynthesis origin of the light elements [46].

The abundance of light elements for any r-sphere may be calculated using the power of the Universe as a function of time (Eq. (32.161)) and the stellar nucleosynthesis rates. During the contraction phase of the oscillatory cycle, the electron neutrino causes neutron production from a photon. Planck's equation and special and general relativity define the mass of the neutron in terms of the spacetime metric as given in the Quarks section. The Planck equation energy, which is equal to the mass energy, applies for the proper time of the neutron given by general relativity (Eq. (32.38)) that is created with the transition of a photon to a neutron.

As discussed previously in the Quantum Gravity of Fundamental Particles section, ordinarily, a photon gives rise to a particle and an antiparticle. The event must be spacelike or annihilation would occur. The event must also conserve energy, momentum, charge, and satisfy the condition that the speed of light is a constant maximum. Eqs. (32.14-32.17) give the relationship whereby matter causes relativistic corrections to spacetime that determines the curvature of spacetime and is the origin of gravity. To satisfy the boundary conditions, particle production from a single photon requires the production of an antimatter particle as well as a particle. The transition state from a photon to a particle and antiparticle comprises two concentric orbitspheres called transition state orbitspheres. The gravitational effect of a spherical shell on an object outside of the radius of the shell is equivalent to that of a point of equal mass at the origin. Thus, the proper time of the concentric orbitsphere with radius ${}^{+}r^{*}$ (the radius is infinitesimally greater than that of the inner transition state orbitsphere with radius r^{*}) is given by the Schwarzschild metric, Eq. (32.38). The proper time applies to each point on the orbitsphere. Therefore, consider a general point in the xy-plane having $r = \lambda\!\!\!^{-}_{C}$; $dr = 0$; $d\theta = 0$; $\sin^2\theta = 1$. Substitution of these parameters into Eq. (32.38) gives

$$d\tau = dt\left(1 - \frac{2Gm_0}{c^2 r_\alpha^*} - \frac{v^2}{c^2}\right)^{\frac{1}{2}} \tag{32.169}$$

with $v^2 = c^2$, Eq. (32.169) becomes

$$\tau = ti\sqrt{\frac{2GM}{c^2 r_\alpha^*}} = ti\sqrt{\frac{2GM}{c^2 \lambda\!\!\!^{-}_{c}}} \tag{32.170}$$

The coordinate time is imaginary because particle/antiparticle production is spacelike. The left-hand side of Eq. (32.170) represents the proper time of the particle/antiparticle as the photon orbitsphere becomes matter. The right-hand side of Eq. (32.170) represents the correction to the laboratory coordinate metric for time corresponding to the curvature of spacetime by the particle production event.

In contrast to the familiar particle production event involving production of particles in matter-antimatter pairs, it is possible to form a particle without production of the corresponding antimatter partner. During the contraction phase, electron neutrinos cause neutron production from photons. In this case, the event must also be spacelike or annihilation would occur. Similarly, the event must also conserve energy, momentum, charge, and satisfy the condition that the speed of light is a constant maximum. Eqs. (32.14-32.17) also apply. They give the relationship whereby matter causes relativistic corrections to spacetime that determines the curvature of spacetime and is the origin of gravity.

The electron neutrino is a special type of photon as given in the Neutrino section which like the photon has zero rest mass and travels at the speed of light. In addition, neutrinos have spin which must be conserved. To satisfy the boundary conditions, particle production from an electron neutrino and a photon requires the production of a single neutral particle, a neutron. In this case, the transition state only comprises a single transition state orbitsphere. The left-hand side of Eq. (32.170) represents the proper time of the neutron as the photon orbitsphere becomes matter. The right-hand side of Eq. (32.170) represents the correction to the laboratory coordinate metric for time corresponding to the relativistic correction of spacetime by the particle production. Thus, ***during the contraction phase of the oscillatory cycle, the electron neutrino causes neutron production from a photon, and the production of protons and electrons occurs by neutron beta decay***.

Typically, antimatter and matter are created in the laboratory in equal amounts; yet, ***celestial antimatter is not observed***. The reason is that electron neutrinos of only one type (electron neutrinos) exist at the initiation of spacetime contraction. Thus, spin conservation requires that antineutron production does not occur as a separate symmetrical reaction, and particle production from a neutrino and a photon prohibits production of the antimatter twin. From Eq. (38.6), the neutron mass is

$$m_{addu\ \ calculated} = (3)(2\pi)\left(\frac{1}{1-\alpha}\right)\left(\frac{2\pi h}{\sec\ c^2}\right)^{\frac{1}{2}}\left(\frac{2\pi(3)ch}{2G}\right)^{\frac{1}{4}} = 1.674\ X\ 10^{-27}\ kg \tag{32.171}$$

The neutron production reaction and the nuclear reaction for the beta decay of a neutron are

$$\gamma + \nu_e \rightarrow {}^1n$$

$$^1n \rightarrow {}^1H + \beta + \overline{\nu}_e + 0.7835\ MeV \tag{32.172}$$

where ν_e is the electron neutrino and $\overline{\nu}_e$ is the electron antineutrino. Eq. (32.172) predicts an electron neutrino background which could account for the atmospheric neutrino anomaly [48]. From Eq. (32.172), ***the number of electrons exactly balances the number of protons.*** **Thus,** ***the Universe is electrically neutral***.

Thus, the Universe is oscillatory in matter, energy, and spacetime without the existence of antimatter due to conservation of spin of the electron neutrino and the relationship of particle production to spacetime contraction. During the expansion phase, ***the arrow of time***

runs forward to lower mass and higher entropy states; whereas, during collapse, ***the arrow of time runs backwards*** relative to the case of the Universe in a state of expansion. Recent particle physics experiments demonstrate that the decay of kaons and antikaons follows a law that is not symmetric with respect to time reversal [39]. The data reveals that there is a microscopic arrow of time, in addition to the thermodynamic and cosmological arrows.

The Universe evolves to higher mass and lower entropy states. Thus, biological organisms such as humans, which rely on the spontaneity of chemical reactions with respect to the forward arrow of time cannot exist in the contracting phase of the Universe. And, compared to the period of the Universe, the ***origins of life*** occurred at a time very close to the beginning of the expansion of the Universe when the direction of the spontaneity of reactions changed to the direction of increasing entropy and the rate of the increase in entropy of the Universe was a maximum.

The origin of the microwave background radiation (CMBR) as the power from the Universe rather than from a Big Bang creation event is demonstrated by the absence of the shadows in the CMBR required for the Big Bang model [36]. As shown in the Power Spectrum of the Cosmic Microwave Background section, when the Universe reaches the maximum radius of the time harmonic variation in the radius of the Universe, (Eq. (32.150)), it is entirely radiation filled. Since the photon has no gravitational mass, the radiation is uniform. As energy converts into matter the power of the Universe may be considered negative for the first quarter cycle starting from the point of maximum expansion as given by Eq. (32.195), and spacetime contracts according to Eq. (32.140). The gravitational field from particle production travels as a light wave front. As the Universe contracts to a minimum radius, the gravitational radius given by Eq. (32.147), constructive interference of the gravitational fields occurs. The resulting slight variations in the density of matter are observed from our present r-sphere. As shown in the Power Spectrum of the Cosmic Microwave Background section, the cosmic microwave background radiation is an average temperature of 2.725 K, with deviations of 30 or so μK in different parts of the sky representing these slight variations in the density of matter. By this mechanism, the production of particles over time from a photon-filled Universe gave rise to centers that eventually aggregated by gravitational attraction into a hierarchy of more massive structures to eventually form the large-scale structure of the cosmos.

Galaxies formed during the collapsing stage of the evolution of the Universe wherein the mass perturbations occurred due to gravity wave interference as demonstrated by the DASI and WMAP data as shown in the Power Spectrum of the Cosmic Microwave Background section. These perturbations resulted in collapsing gas clouds that formed quasars. Then each of these quasars erupted into a supernova and formed a blackhole. The expelled gas eventually formed galaxies. The observation of a blackhole in the center of each galaxy is consistent with the origin of galaxies from a quasar supernova [49, 50]. Furthermore, since angular momentum must be conserved in the rotation of the founding quasar and the resulting blackhole and galactic rotating stars, a linear relationship of the plot of the velocity of the outer stars of given galaxy to the blackhole mass is expected. This ratio called sigma is indeed observed to be linear [49, 50].

The Universe is oscillatory with a finite minimum radius, the gravitational radius. Thus, stellar and celestial structures evolve on a time scale that is greater than the observed time of expansion. ***Stars exist which are older than the elapsed time of the present expansion*** as stellar evolution occurred during the contraction phase [51, 52]. Galaxy evolution also occurred during the contraction phase as revealed by high-redshift radio galaxies and galaxies associated with extremely distant, luminous quasars that date back to the beginning of the expansion [46, 47].

The Gemini Deep Deep Survey confirmed the predicted existence of old galaxies at the beginning of the expansion at 10 billion light years and further directly disprove the Big Bang theory of cosmology [53-55]. These results were confirmed by a spectroscopic redshift survey that probed the most massive and quiescent galaxies back at 10 billion light years [56, 57]. It was found that a significant fraction of the massive old galaxies observed over all of time since the expansion were in place in the early Universe. This is also shown by the Hubble Ultra Deep Field (HUDF) given in Figure 32.10. Recently, a definitive validation of the classical predictions was provided by the Keck survey for gravitationally lensed Lyα emitters that found galaxies back at over 13 billion light years [58].

Figure 32.10. The Hubble Ultra Deep Field (HUDF) shows mature galaxies at the time of the beginning of the expansion of the Universe. The "Big Bang" is NOT observed. This image is a composite of two separate images taken by the Hubble's Advanced Camera for Surveys (ACS) and the Near Infrared Camera and Multiobject Spectrometer (NICMOS), the result of over eleven and a half days of exposure. It contains an estimated ten thousand galaxies. Released on 9 March 2004. Courtesy of NASA, ESA, S. Beck with STScI and the HUDF Team.

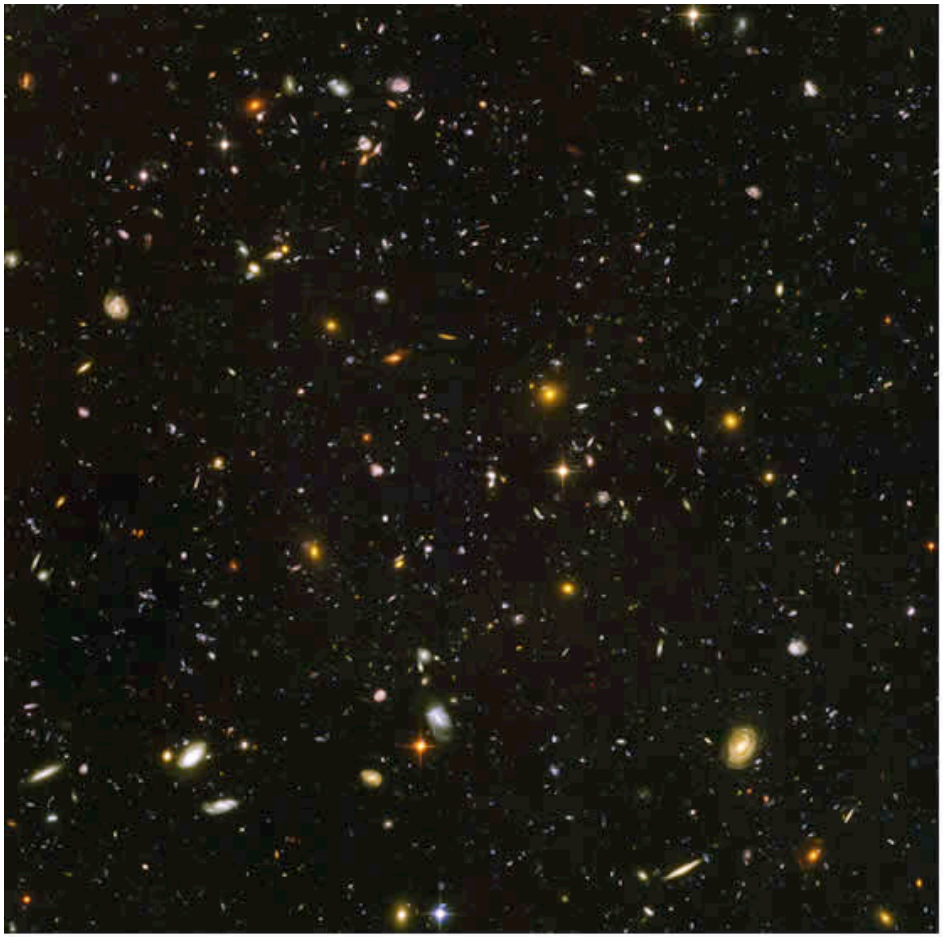

In addition to fusion reactions in stars, hydrino transitions to lower energy hydrino states is a source of power contribution to the CMBR as well as a source of spacetime expansion as matter is converted into energy. As given in the Disproportionation of Energy States section,

classical physical laws predict that atomic hydrogen may undergo a catalytic reaction with certain species, including itself, that can accept energy in integer multiples of the potential energy of atomic hydrogen, $m \cdot 27.2$ eV, wherein m is an integer. The predicted reaction involves a resonant, nonradiative energy transfer from otherwise stable atomic hydrogen to the catalyst capable of accepting the energy. The product is H(1/p), fractional Rydberg states of atomic hydrogen called "hydrino atoms," wherein n = 1/2, 1/3, 1/4,…, 1/p ($p \leq 137$ is an integer) replaces the well-known parameter n = integer in the Rydberg equation for hydrogen excited states. Each hydrino state also comprises an electron, a proton, and a photon, but the field contribution from the photon increases the binding energy rather than decreasing it corresponding to energy desorption rather than absorption. Since the potential energy of atomic hydrogen is 27.2 eV, $m\ H$ atoms serve as a catalyst of $m \cdot 27.2\ eV$ for another $(m+1)$th H atom (See BlackLight Process section). For example, a H atom can act as a catalyst for another H by accepting 27.2 eV from it via through-space energy transfer such as by magnetic or induced electric dipole-dipole coupling to form an intermediate that decays with the emission of continuum bands with short wavelength cutoffs and energies of $m^2 \cdot 13.6\ eV$ $\left(\frac{91.2}{m^2}\ nm\right)$. The continuum radiation band at 10.1 nm and going to longer wavelengths for theoretically predicted transitions of H to lower-energy, so called "hydrino" state H(1/4), was observed only arising from pulsed pinch gas discharges comprising some hydrogen and oxygen as an oxide, first at BlackLight Power, Inc. (BLP) and reproduced at the Harvard Center for Astrophysics (CfA) [59-64]. HOH was shown to be the catalyst in these pinch plasma continua as well as in the 10-30 nm EUV continuum observed from plasma having essentially no field. The latter plasma was formed by igniting a solid fuel source of H and HOH catalyst by passing a ultra-low voltage, high current through the fuel to produce explosive plasma [59]. Moreover, $m\ H$ catalyst (Eqs. (5.48-5.61)) was identified to be active in astronomical sources such as the Sun, stars, and interstellar medium wherein the characteristics of hydrino product match those of the dark matter of the Universe [59]. Hydrogen continua from transitions to form hydrinos matches the emission from white dwarfs, provides a possible mechanism of linking the temperature and density conditions of the different discrete layers of the coronal/chromospheric sources, and provides a source of the diffuse ubiquitous EUV cosmic background with the 10.1 nm continuum matching the observed intense 11.0-16.0 nm band in addition to resolving other cosmological mysteries [59,63,65,66]. Given the seeding by the anisotropic gravitational forces in a contracting Universe, expansion of the Universe depends on the rate of energy release, which varies throughout the Universe; thus, clusters of galaxies, huge voids, and other ***large features which are observed*** [67-71] are caused by the interaction between the rate of energy release with concomitant spacetime expansion and gravitational attraction. Hydrogen-type atoms and molecules comprise most of the matter of the Universe. The distinction between hydrogen and hydrinos with respect to the interaction with electromagnetic radiation and release of energy by transitioning to lower energy states (See Disproportionation of Energy States section) also has an influence on the formation of large voids and walls of matter. Lower-energy atomic hydrogen atoms, hydrinos, each have the same mass and a similar interaction as the neutron. According to Steinhardt and Spergel of Princeton University [72], these are the properties of dark matter that are necessary in order for the theory of the structure of galaxies to work out on all scales. The observation that galaxy clusters arrange themselves as predicted for cold dark matter except that the cores are less dense than expected is explained. Hydrinos further account for the observation

that small halos of dark matter are evaporated when they approach larger ones and that dark matter is easily influenced by black holes, explaining how they grew so large.

Laboratory EUV continuum results [59] offer resolution to many otherwise inexplicable celestial observations with (a) the energy and radiation from the hydrino transitions being the source of extraordinary temperatures and power regarding the solar corona problem, the cause of sunspots and other solar activity, and why the Sun emits X-rays [63], (b) the hydrino-transition radiation being the radiation source heating the WHIM and behind the observation that diffuse Hα emission is ubiquitous throughout the Galaxy requiring widespread sources of flux shortward of 912 $\mathring{A}$, and (c) the identity of dark matter being hydrinos.

Stars also comprise plasmas of hydrogen with surfaces comprised of essentially dense atomic hydrogen permissive of multi-body H interactions to propagate transition of H to H(1/(m +1) wherein $m\ H$ serves as the catalyst. Such transitions are predicted to emit EUV continuum radiation according to Eqs. (5.48-5.61). The emission from white dwarfs arising from an extremely high concentration of hydrogen is modeled as an optically thick blackbody of ~ 50,000 K gas comprising predominantly hydrogen and helium. A modeled composite spectrum of the full spectral range from 10 nm to >91.2 nm with an abundance He/H=10^{-5} from Barstow and Holberg [65] is shown in Figure 10 of Ref. [59]. Albeit, while white dwarf spectra can be curve fitted using stratification and adjustable He and H column densities and ionization fractions to remove some inconsistencies between optical and EUV spectra [73] and independent measurements of the latter, matching the spectrum at the short-wavelengths is problematic. Alternatively, combining the laboratory-observed emission continuum bands gives a spectrum with continua having edges at 10.1 nm, 22.8, nm, and 91.2 nm, a match to the white dwarf spectrum [59]. However, the proposed nature of the plasmas and the mechanisms are very different. The emission in our studies is assigned to hydrino transitions in cold-gas, optically-thin plasmas absent any helium. White-dwarf and celestial models may need revision and benefit from our discovery of high-energy H continua emission.

For example, there is no existing physical model that can couple the temperature and density conditions in different discrete regions of the outer atmosphere (chromosphere, transition region, and corona) of coronal/chromospheric sources [73]. Typically the corona is modeled to be three orders of magnitude hotter than the surface that is the source of coronal heating seemingly in defiance of the second law of thermodynamics. Reconciliation is offered by the mechanism of line absorption and re-emission of the $m^2 \cdot 13.6\ eV$ (Eq. (5.57)) continuum radiation. The 91.2 nm continuum to longer wavelengths is expected to be prominent (less attenuated than the 10.1 nm and 22.8 nm bands) and is observed in the solar extreme ultraviolet spectrum as shown in Figure 11 of Ref. [59] and Ref. [74] despite attenuation by the coronal gas. High-energy-photon excitation is more plausible than a thermal mechanism with T~10^6 given the 4000 K surface temperature and the observation of the CO absorption band at 4.7 μm in the solar atmosphere wherein CO cannot exist above 4000 K [75]. Considering the 10.1 nm band as a source, the upper limit of coronal temperature based on excitation of about 10^6 K is an energy match. In addition to the temperature, another extraordinary observation is that although the total average energy output of the outer layers of the Sun is $\cong 0.01\ \%$ of the photospheric radiation, local transient events can produce an energy flux that exceeds the photospheric flux [76]. The energy source of the latter may be magnetic in nature, but identity of the highly ionizing coronal source is not established. Nor, has the total energy balance of the Sun been reconciled. The possibility of a revolutionary discovery of a new source of energy in the Sun based on a prior undiscovered process is an open question [77]. That $m\ H$ catalyzed hydrino

transitions occur in stars and the Sun [78] as evident by corresponding continua in its spectrum resolves the solar corona problem, the cause of sunspots and other solar activity, and why the Sun emits X-rays [63].

The laboratory EUV continuum results [59] have further implications for the resolution of the identity of dark matter and the identity of the radiation source behind the observation that diffuse Hα emission is ubiquitous throughout the Galaxy and widespread sources of flux shortward of 912 $\AA$ are required [79]. The identity of dark matter has been a cosmological mystery. It is anticipated that the emission spectrum of the extreme ultraviolet background of interstellar matter possesses the spectral signature of dark matter. Labov and Bowyer designed a grazing incidence spectrometer to measure and record the diffuse extreme ultraviolet background [79]. The instrument was carried aboard a sounding rocket, and data were obtained between 80 $\AA$ and 650 $\AA$ (data points approximately every 1.5 $\AA$). Several lines including an intense 635 $\AA$ emission associated with dark matter were observed [79] which has considerable astrophysical importance as indicated by the authors:

> "Regardless of the origin, the 635 $\AA$ emission observed could be a major source of ionization. Reynolds (1983, 1984, 1985) has shown that diffuse Hα emission is ubiquitous throughout the Galaxy, and widespread sources of flux shortward of 912 $\AA$ are required. Pulsar dispersion measures (Reynolds 1989) indicate a high scale height for the associated ionized material. Since the path length for radiation shortward of 912 $\AA$ is low, this implies that the ionizing source must also have a large scale height and be widespread. Transient heating appears unlikely, and the steady state ionization rate is more than can be provided by cosmic rays, the soft X-ray background, B stars, or hot white dwarfs (Reynolds 1986; Brushweiler & Cheng 1988). Sciama (1990) and Salucci & Sciama (1990) have argued that a variety of observations can be explained by the presence of dark matter in the galaxy which decays with the emission of radiation below 912 $\AA$.
>
> The flux of 635 $\AA$ radiation required to produce hydrogen ionization is given by $F = \zeta_H / \sigma_\lambda = 4.3\ X\ 10^4\ \zeta_{-13}\ photons\ cm^{-2}s^{-1}$, where ζ_{-13} is the ionizing rate in units of $10^{-13}s^{-1}$ per H atom. Reynolds (1986) estimates that in the immediate vicinity of the Sun, a steady state ionizing rate of ζ_{-13} between 0.4 and 3.0 is required. To produce this range of ionization, the 635 $\AA$ intensity we observe would have to be distributed over 7% - 54% of the sky."

The 63.5 ± 0.47 nm line [79] matches a hydrino transition predicted for H undergoing catalysis with H (m=1) as the catalyst giving rise to a concerted energy exchange of the total energy of 40.8 eV with the excitation of the He $1s^2$ to $1s^12p^1$ transition. The predicted 63.3 nm emission associated with dark matter was observed with the addition of hydrogen to helium microwave plasma as shown previously [63,80]. An alternative assignment suggested by Labov and Bowyer [79] is the 63.0 nm line of O V requiring a large-scale non-thermal source of ionization. Continuum radiation from transitions to low-level hydrino states can provide this radiation. Indeed, the observation of the 63.3 nm line is also associated with the presence of an interstellar X-ray background.

The first soft X-ray background was detected and reported [81] about 25 years ago. Quite naturally, it was assumed that these soft X-ray emissions were from ionized atoms within hot gases. Labov and Bowyer also interpreted the data as emissions from hot gases. However,

the authors left the door open for some other interpretation with the following statement from their introduction:

> "It is now generally believed that this diffuse soft X-ray background is produced by a high-temperature component of the interstellar medium. However, evidence of the thermal nature of this emission is indirect in that it is based not on observations of line emission, but on indirect evidence that no plausible non-thermal mechanism has been suggested which does not conflict with some component of the observational evidence."

The authors also state "if this interpretation is correct, gas at several temperatures is present." Specifically, emissions were attributed to gases in three ranges: $5.5 < \log T < 5.7$; $\log T = 6$; $6.6 < \log T < 6.8$. Observations in the ultraviolet with HST and FUSE [82] and also XMM-Newton [83] confirm these extraordinary temperatures of diffuse intergalactic medium (IGM) and reveal that a large component of the baryonic matter of the Universe is in the form of WHIM (warm-hot ionized media) [82,83]. The mysteries of the identity of dark matter, the observed dark interstellar medium spectrum, the source of the diffuse X-ray background, and the source of ionization of the IGM [82,83] are resolved by the formation of hydrinos that emit EUV and X-ray continua depending on the state transition and conditions; the continua create highly ionized ions that emit ion radiation of non-thermal origin; the hydrino transition H to H(1/2) results in a 63.3 nm line [63,80], and He^+ acting as a catalyst of 54.4 eV ($2 \cdot 27.2\ eV$) pumps the intensity of helium ion lines such as the 30.4 nm line [61,63].

Evidence for EUV emission from hydrino transitions also comes from interstellar medium (ISM) since it provides a source of the diffuse ubiquitous EUV cosmic background. Specifically, the 10.1 nm continuum matches the observed intense 11.0-16.0 nm band [65,66]. Furthermore, it provides a mechanism for the high ionization of helium of the ISM and the excess EUV radiation from galaxy clusters that cannot be explained thermally [84]. Moreover, recent data reveals that X-rays from distant active galactic nuclei sources are absorbed selectively by oxygen ions in the vicinity of the galaxy [85]. The temperature of the absorbing halo is between 1 million and 2.5 million Kelvin, or a few hundred times hotter than the surface of the Sun. The corresponding energy range is 86 eV to 215 eV which is in the realm of the energy released for the transition of H to H(1/4). Additional astrophysical evidence such as the observation that a large component of the baryonic matter of the Universe is in the form of WHIM (warm-hot ionized media) in the absence of a conventional source and the match of hydrinos to the identity of dark matter was presented previously [63]. The latter case is further supported by observations of signature electron-positron annihilation energy.

Dark matter comprises a majority of the mass of the Universe as well as intra-galactic mass [86,87]. It would be anticipated to concentrate at the center of the Milky Way galaxy due to the high gravity from the presence of a super massive blackhole at the center that emits gamma rays as matter falls into it. Since hydrinos are each a state of hydrogen having a proton nucleus, high-energy gamma rays impinging on dark matter will result in pair production. The characteristic signature of the identity of dark matter as hydrino being the emission of the 511 keV annihilation energy of pair production is observed [88-90]. Another hydrino decay pathway for this radiation is given by Eq. (32.173). Interstellar medium [91-93], gamma-ray bursts [93,94], and solar flares [75,93,95] also emit 511 keV line radiation. The dominant source of positrons in gamma-ray bursts is likely pair production by photon on photons or on strong magnetic fields [93]. The solar-flare emission is likely due to production of radioactive positron

emitters in accelerated charge interactions [93]; whereas, the diffuse 511 keV radiation by interstellar medium is consistent with the role of hydrino as dark matter in pair production from incident cosmic radiation [91-93].

The characteristic spectral signatures and properties of hydrino match those attributed to the dark matter of the Universe. The Universe is predominantly comprised of hydrogen and a small amount of helium. These elements exist in interstellar regions of space, and they are expected to comprise the majority of interstellar matter. However, the observed constant angular velocity of many galaxies as the distance from the luminous galactic center increases can only be accounted for by the existence of nonluminous weakly interacting matter, dark matter. It was previously accepted that dark matter exists at the cold fringes of galaxies and in cold interstellar space. This has since been disproved by the observation of Bournaud et al. [86,87] that demonstrated that galaxies are mostly comprised of dark matter, and the data persistently supports that dark matter probably accounts for the majority of the universal mass.

The best evidence yet for the existence of dark matter is its direct observation as a source of massive gravitational mass evidenced by gravitational lensing of background galaxies that does not emit or absorb light as shown in as shown in Figure 32.11 [96]. There has been the announcement of some unexpected astrophysical results that support the existence of hydrinos. In 1995, Mills published the GUTCP prediction [97] that the expansion of the Universe was accelerating from the same equations that correctly predicted the mass of the top quark before it was measured. To the astonishment of cosmologists, this was confirmed by 2000. Mills made another prediction about the nature of dark matter based on GUTCP that may be close to being confirmed. Bournaud et al. [86,87] suggest that dark matter is hydrogen in dense molecular form that somehow behaves differently in terms of being unobservable except by its gravitational effects. Theoretical models predict that dwarfs formed from collisional debris of massive galaxies should be free of nonbaryonic dark matter. So, their gravity should tally with the stars and gas within them. By analyzing the observed gas kinematics of such recycled galaxies, Bournaud et al. [86,87] have measured the gravitational masses of a series of dwarf galaxies lying in a ring around a massive galaxy that has recently experienced a collision. Contrary to the predictions of Cold-Dark-Matter (CDM) theories, their results demonstrate that they contain a massive dark component amounting to about twice the visible matter. This baryonic dark matter is argued to be cold molecular hydrogen, but it is distinguished from ordinary molecular hydrogen in that it is not traced at all by traditional methods, such as emission of CO lines. These results match the predictions of the dark matter being molecular hydrino.

Figure 32.11. Dark matter ring in galaxy cluster. This Hubble Space Telescope composite image shows a ghostly "ring" of dark matter in the galaxy cluster Cl 0024+17. The ring is one of the strongest pieces of evidence to date for the existence of dark matter, a prior unknown substance that pervades the Universe. Courtesy of NASA, M.J. Jee and H. Ford (Johns Hopkins University).

Additionally, astronomers Jee at al. [98] using data from NASA's Hubble Telescope have mapped the distribution of dark matter, galaxies, and hot gas in the core of the merging galaxy cluster Abell 520 formed from a violent collision of massive galaxy clusters and have determined that the dark matter had collected in a dark core containing far fewer galaxies than would be expected if dark matter was collsionless with dark matter and galaxies anchored together. The collisional debris left behind by the galaxies departing the impact zone behaved as hydrogen did, another indication that the identity of dark matter is molecular hydrino. Moreover, detection of alternative hypothesized identities for dark matter such as super-symmetry particles such as neutalinos has failed at the Large Hadron Collider; nor, has a single event been observed for weakly interacting massive particles or wimps at the Large Underground Xenon (LUX) experiment [99].

During the expansion phase, protons and electrons of hydrinos which comprises the dark matter annihilate to photons and electron neutrinos as given in the New "Ground" State section. To conserve spin (angular momentum) the reaction is

$$\bar{\nu}_e + {}^1H\left[\frac{a_H}{p}\right] \rightarrow \gamma + \nu_e \tag{32.173}$$

where ν_e is the electron neutrino. (A similar reaction to that of Eq. (32.173) is the reaction of a muon neutrino rather than an electron antineutrino with a hydrino to give a gamma photon and a muon antineutrino.) Disproportionation reactions to the lowest-energy states of hydrogen followed by electron capture with gamma ray emission may be *a source of nonthermal γ-ray bursts from interstellar regions* [100]. A branch of the decay path may also be similar to that of the π^0 meson. Gamma and pair-production decay would result in characteristic 511 keV annihilation energy emission. This emission has been recently been identified with dark matter [101,102].

Furthermore, a very plausible source of nonthermal γ-ray bursts from interstellar regions [100] may be due to conversion of matter to photons of the Planck mass-energy, which may also give rise to cosmic rays. When the gravitational potential energy density of a massive body such as a blackhole equals that of a particle having the Planck mass as given by Eqs. (32.22-32.32), the matter may transition to photons of the Planck mass given by Eq. (32.31). In the case of the Planck mass, the gravitational potential energy (Eq, (32.30)) is equal to the Planck, electric, and magnetic energies which equal mc^2 (Eq. (32.32)), and the coordinate time is equal to the proper time (Eqs. (32.33-32.34) and Eq. (32.43)). However, the particle corresponding to the Planck mass may not form since its gravitational velocity (Eq. (32.33)) is the speed of light. *(The limiting speed of light eliminates the singularity problem of Einstein's equation that arises as the radius of a blackhole equals the Schwarzschild radius. General relativity with the singularity eliminated resolves the paradox of the infinite propagation velocity required for the gravitational force in order to explain why the angular momentum of objects orbiting a gravitating body does not increase due to the finite propagation delay of the gravitational force according to special relativity [103]).* Thus, it remains a photon. Even light from a blackhole will escape when the decay rate of the trapped matter with the concomitant spacetime expansion is greater than the effects of gravity that oppose this expansion. The annihilation of a blackhole may be the source of *g-ray bursts*. Gamma-ray bursts are the most energetic phenomenon known that can release an explosion of gamma rays packing 100 times more energy than a supernova explosion [104]. Cosmic rays are the most energetic particles known, and their origin is also a mystery [105]. In 1966, Cornell University's Kenneth Greisen predicted that interaction with the ubiquitous photons of the cosmic microwave background would result in a smooth power-law cosmic-ray energy spectrum being sharply cutoff close to $5\,X\,10^{19}\ eV$. However, in 1998, Schwarzschild reported [106] that the *Akeno Giant Air Shower Array (AGASA) in Japan has collected data that show the cosmic-ray energy spectrum is extending beyond the Greisen-Zatsepin-Kuzmin (GZK) cutoff.* According to the GZK cutoff, the cosmic spectrum cannot extend beyond $5\,X\,10^{19}\ eV$, but AGASA, the world's largest air shower array, has shown that the spectrum is extending beyond without any clear sign of cutoff. Similarly, the Utah Fly's Eye had detected cosmic rays with energy up to $3\,X\,10^{20}\ eV$ [107,108]. *Photons, each of the Planck mass, may be the source of these inexplicably energetic cosmic rays* corresponding to tremendous power and concomitant spacetime expansion.

POWER SPECTRUM OF THE COSMOS

The maximum energy release of the Universe given by Eq. (32.142) occurred at the beginning of the expansion phase, and the power spectrum is a function of the r-sphere of the observer. The power spectrum of the cosmos, as measured by the Las Campanas survey, generally follows the prediction of cold dark matter on the scales of 200 million to 600 million light-years. However, the power increases dramatically on scales of 600 million to 900 million light-years [50]. This discrepancy means that the Universe is much more structured on those scales than current theories can explain. The Universe is oscillatory in matter/energy and spacetime with a finite minimum radius. The minimum radius of the Universe, 300 billion light years [32], is larger than that provided by the current expansion, approximately 10 billion light years [28]. The Universe is a four-dimensional hyperspace of constant positive curvature at each r-sphere. The coordinates are spherical, and the space can be described as a series of spheres each of constant radius r whose centers coincide at the origin. The existence of the mass m_U causes the area of the spheres to be less than $4\pi r^2$ and causes the clock of each r-sphere to run so that it is no longer observed from other r-spheres to be at the same rate. The Schwarzschild metric given by Eq. (32.38) is the general form of the metric that allows for these effects. Consider the present observable Universe that has undergone expansion for 10 billion years. The radius of the Universe as a function of time from the coordinate r-sphere is of the same form as Eq. (32.153). The average size of the Universe, r_U, is given as the sum of the gravitational radius, r_g, and the observed radius, 10 billion light years.

$$r_U = r_g + 10^{10} \ light\ years$$

$$r_U = 3.12\ X\ 10^{11} \ light\ years + 10^{10} \ light\ years \tag{32.174}$$

$$r_U = 3.22\ X\ 10^{11} \ light\ years$$

The frequency of Eq. (32.153) is one half the amplitude of spacetime expansion from the conversion of the mass of Universe into energy according to Eq. (32.140). Thus, keeping the same relationships, the frequency of the current expansion function is the reciprocal of one half the current age. Substitution of the average size of the Universe, the frequency of expansion, and the amplitude of expansion, 10 billion light years, into Eq. (32.153) gives ***the radius of the Universe as a function of time for the coordinate r-sphere***.

$$\aleph = \left(3.22\ X\ 10^{11}\ light\ years - 1\ X\ 10^{10}\ \cos\left(\frac{2\pi t}{5\ X\ 10^{9}\ light\ years} \right) \right) light\ years \tag{32.175}$$

The Schwarzschild metric gives the relationship between the proper time and the coordinate time (Eq. (32.38)). The infinitesimal temporal displacement, $d\tau^2$, is

$$d\tau^2 = \left(1 - \frac{2Gm_U}{c^2 r} \right) dt^2 - \frac{1}{c^2} \left[\left(\frac{dr^2}{1 - \frac{2Gm_U}{c^2 r}} \right) + r^2 d\theta^2 + r^2 \sin^2\theta d\phi^2 \right] \tag{32.176}$$

In the case that $dr^2 = d\theta^2 = d\phi^2 = 0$, the relationship between the proper time and the coordinate time is

$$d\tau^2 = \left(1 - \frac{2Gm_U}{c^2 r}\right) dt^2 \tag{32.177}$$

$$\tau = t\sqrt{1 - \frac{2Gm_U}{c^2 r}} \tag{32.178}$$

$$\tau = t\sqrt{1 - \frac{r_g}{r}} \tag{32.179}$$

The maximum power radiated by the Universe is given by Eq. (32.142) and occurs when the proper radius, the coordinate radius, and the gravitational radius r_g are equal. For the present Universe, the coordinate radius is given by Eq. (32.174). The gravitational radius is given by Eq. (32.147). The maximum of the power spectrum of a trigonometric function occurs at its frequency [109]. Thus, the coordinate maximum power according to Eq. (32.175) occurs at $5\,X\,10^9\ light\ years$. The maximum power corresponding to the proper time is given by the substitution of the coordinate radius, the gravitational radius r_g, and the coordinate power maximum into Eq. (32.179). The power maximum in the proper frame occurs at

$$\tau = 5\,X\,10^9\ light\ years\sqrt{1 - \frac{3.12\,X\,10^{11}\ light\ years}{3.22\,X\,10^{11}\ light\ years}} \tag{32.180}$$

$$\tau = 880\,X\,10^6\ light\ years$$

The power maximum of the current observable Universe is predicted to occur on the scale of $880\,X\,10^6\ light\ years$. There is excellent agreement between the predicted value and the experimental value of between 600 million to 900 million light years [110].

THE DIFFERENTIAL EQUATION OF THE RADIUS OF THE UNIVERSE

The differential equation of the radius of the Universe, $\aleph$, can be derived as a conservative simple harmonic oscillator having a restoring force, $\mathbf{F}$, which is proportional to the radius. The proportionality constant, k, is given in terms of the potential energy, E, gained as the radius decreases from the maximum expansion to the minimum contraction.

$$\frac{E}{\aleph^2} = k \tag{32.181}$$

The Universe oscillates between a minimum and maximum radius as matter is created into energy and then energy is converted to matter. At the minimum radius, the gravitational velocity, v_G, is given by Eq. (32.33) and the gravitational radius r_G, is given by Eq. (32.22) wherein an electromagnetic wave of mass energy equivalent to the mass of the Universe travels in a circular orbit wherein the eccentricity is equal to zero (Eq. (35.21)), and the escape velocity from the Universe can never be reached. At this point in time, all of the energy of the Universe

is in the form of matter, and the gravitational energy (Eq. (32.148)) is equal to $m_U c^2$. Thus, the proportionality constant of the restoring force with respect to the radius is

$$F = -k\aleph = -\frac{m_U c^2}{r_G^2}\aleph = -\frac{m_U c^2}{\left(\frac{Gm_U}{c^2}\right)^2}\aleph \tag{32.182}$$

Considering the oscillation, the differential equation of the radius of the Universe, $\aleph$, follows from Eq. (32.182) as given by Fowles [111].

$$\begin{aligned} m_U \ddot{\aleph} + \frac{m_U c^2}{r_G^2}\aleph &= 0 \\ m_U \ddot{\aleph} + \frac{m_U c^2}{\left(\frac{Gm_U}{c^2}\right)^2}\aleph &= 0 \end{aligned} \tag{32.183}$$

The solution of Eq. (32.183) which gives the radius of the Universe as a function of time follows from Fowles [111].

$$\begin{aligned} \aleph &= \left(r_g + \frac{cm_U}{Q}\right) - \frac{cm_U}{Q}\cos\left(\frac{2\pi t}{\frac{2\pi r_G}{c}}\right) \\ \aleph &= \left(\frac{2Gm_U}{c^2} + \frac{cm_U}{\frac{c^3}{4\pi G}}\right) - \frac{cm_U}{\frac{c^3}{4\pi G}}\cos\left(\frac{2\pi t}{\frac{2\pi Gm_U}{c^3}}\right) \end{aligned} \tag{32.184}$$

The gravitation force causes the radius of Eq. (32.184) to be offset [111]. After Eq. (32.38), the force equations of general relativity give the offset radius, r_U. The minimum radius corresponds to the gravitational radius r_g whereby the proper time is equal to the coordinate time. The offset radius, r_U, is

$$r_U = r_g + \frac{cm_U}{\frac{c^3}{4\pi G}} \tag{32.185}$$

The expansion/contraction rate, $\dot{\aleph}$, is given by taking the derivative with respect to time of Eq. (32.184).

$$\dot{\aleph} = 4\pi c \cdot \sin\left(\frac{2\pi t}{\frac{2\pi Gm_U}{c^3}}\right) \tag{32.186}$$

According to special relativity no signal may travel faster than c, the speed of light for any observer. The maximum expansion rate for a 3-sphere is $4\pi c$ which is given in Eq. (32.186). The expansion/contraction acceleration, $\ddot{\aleph}$, is given by taking the derivative with respect to time of Eq. (32.186).

$$\ddot{\aleph} = 2\pi \frac{c^4}{Gm_U} \cdot \cos\left(\frac{2\pi t}{\frac{2\pi G m_U}{c^3}} \right) \tag{32.187}$$

The Universe oscillates between the extremes of all matter and all energy. At the beginning of its expansion, the Universe is all matter with no electromagnetic radiation; thus, ***the Universe is not observable for earlier times***. The observer's light sphere determines the limits of observation thereafter. Furthermore, ancient stars and the large-scale structure of the cosmos comprising galactic superclusters and voids that could not have formed within the elapsed time of expansion are visible [50-57,67-71,112,113]. Recently, a uniform cosmic infrared background has been discovered which is consistent with the heating of dust with reradiation over a much longer period than the elapsed time of expansion [114]. The size of the Universe may be detected by observing the early curvature, the power spectrum, and the microwave background temperature. In the latter case, the power released as a function of time over the entire Universe is given by Eq. (32.161). The size of the Universe as a function of time is given by Eq. (32.153). The microwave background temperature corresponds to the power density over the entire Universe that is to within a few parts per million uniform on the scale of the entire Universe. Thus, the microwave background temperature as a function of time for each observer within his light sphere is given by Eq. (32.168).

The Hubble constant is given by the ratio of the expansion rate (Eq. (32.186)) given in units of $\frac{km}{\sec}$ and the radius of the expansion (Eq. (32.126)) in units of Mpc (1 Megaparsec (Mpc) is $3.258\ X\ 10^6$ light years).

$$H = \frac{\dot{\aleph}}{ct} = \frac{4\pi \sin\left(\frac{2\pi t}{\frac{2\pi G m_U}{c^3}} \right)}{t} \tag{32.188a}$$

Using

$$\begin{aligned} 1\ Gyr = 3.1358\ X\ 10^{16} s &\rightarrow \frac{3.1358\ X\ 10^{16} s}{1\ Gyr} = 1 \\ 1\ Mpc = 3.0857\ X\ 10^{19} km &\rightarrow \frac{3.0857\ X\ 10^{19} km}{1\ Mpc} = 1 \end{aligned} \tag{32.188b}$$

and $t = 10\ Gyr$, Eq. (32.188a) is given by

$$H = \frac{4\pi \sin\left(2\pi \frac{t}{983\ Gyr}\right) \cdot \frac{3.0857\ X\ 10^{19} km}{1\ Mpc}}{t \cdot \frac{3.1358\ X\ 10^{16} s}{1\ Gyr}}$$

$$= 1229 \frac{km}{s \cdot Mpc} \cdot \frac{\sin\left(2\pi \frac{t}{983\ Gyr}\right)}{\frac{t}{1\ Gyr}} \tag{32.188c}$$

$$H\Big|_{t=10\ Gyr} = 1229 \frac{km}{s \cdot Mpc} \cdot \frac{\sin\left(2\pi \frac{10\ Gyr}{983\ Gyr}\right)}{\frac{10\ Gyr}{1\ Gyr}} \approx 78.5 \frac{km}{s \cdot Mpc}$$

The differential in the radius of the Universe $\Delta\aleph$ due to its acceleration is given by

$$\Delta\aleph = 1/2 \ddot{\aleph} t^2 \tag{32.189}$$

The ***expansion of the light sphere due to the acceleration of the expansion of the cosmos*** given by Eq. (32.155) and Eq. (32.187) is shown graphically in Figure 32.12. The observed brightness of supernovae as standard candles is inversely proportional to their distance squared. As shown in Figure 32.12, $\Delta\aleph$ increases by a factor of about three as the time of expansion increases from the midpoint to a time comparable to the elapsed time of expansion, $t = 10^{10}\ light\ years = 3.069\ X\ 10^3\ Mpc$. As an approximation, this differential in expanded radius corresponds to a decease in brightness of a supernovae standard candle of about an order of magnitude of that expected where the distance is taken as $\Delta\aleph$. This result is consistent with the experimental observation [37-39]. Recently, the BOOMERANG telescope [115] imaged the microwave background radiation covering about 2.5% of the sky with an angular resolution of 35 times that of COBE [33]. The image revealed hundreds of complex structures that were visible as tiny fluctuations—typically only 100 millionths of a degree (0.0001 °C)—in temperature of the Cosmic Microwave Background. Structures of about 1° in size were observed that are consistent with a Universe of nearly flat geometry since the commencement of its expansion. The data is consistent with a large offset radius of the Universe as given by Eq. (32.147) with a fractional increase in size (Eq. (32.153)) since the commencement of expansion about 10 billion years ago.

Figure 32.12. The differential expansion of the light sphere due to the acceleration of the expansion of the cosmos as a function of time.

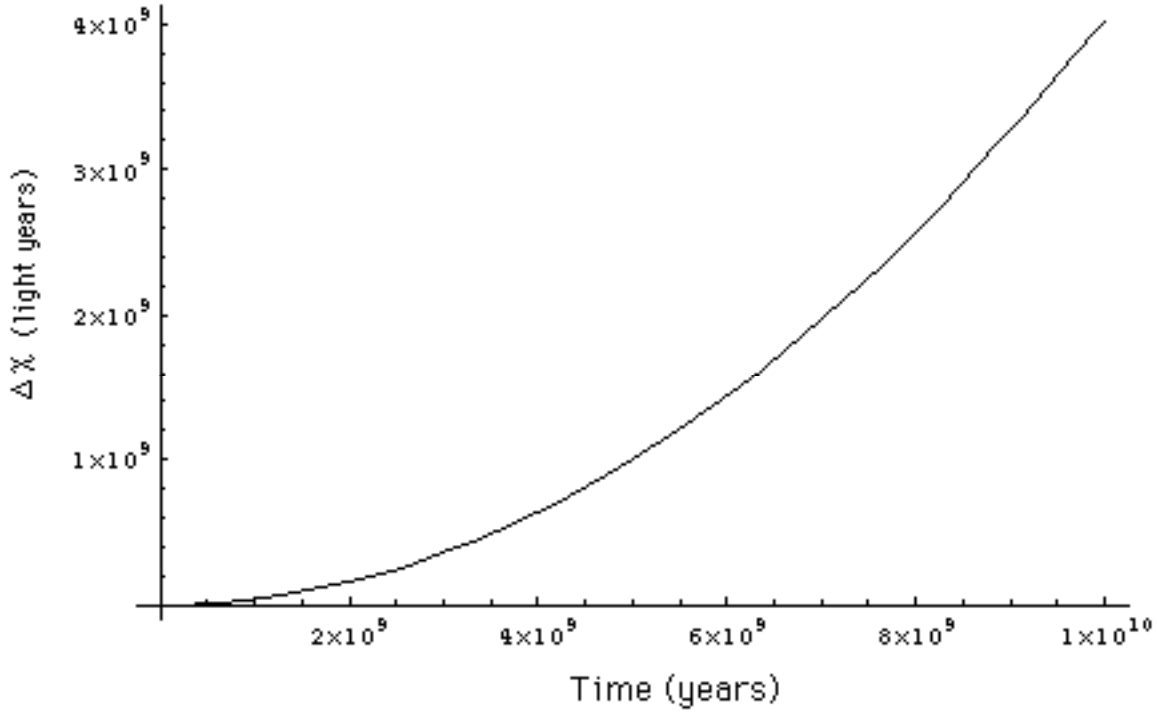

Recently NASA announced Hubble Space telescope results taken on the most distant supernova ever at a distance of 10 billion light years [116,117]. The extraordinary brightness of this standard candle compared to other such closer supernovas indicates that the Universe accelerated from a stationary state 10 billion years ago. This result is in agreement with the predictions of Eqs. (32.15-32.154) and Figure 32.5 presented before 1995 which predated the startling discovery that the Universe is accelerating.

POWER SPECTRUM OF THE COSMIC MICROWAVE BACKGROUND

The cosmic microwave background radiation (CMBR) corresponds to an average temperature of 2.725 K, with deviations of 30 μK or so in different parts of the sky representing slight variations in the density of matter. Early detailed measurements of the anisotropy as well as the discovery of polarization of the CMBR were achieved by the Degree Angular Scale Interferometer (DASI) [35]. The angular power spectrum was measured in the range $100 < \ell < 900$, and peaks in the power spectrum from the temperature fluctuations of the cosmic microwave background radiation appear at certain values of ℓ of spherical harmonics [35]. Peaks were observed at $\ell \approx 200$, $\ell \approx 550$, and $\ell \approx 800$ with relative intensities of 1, 0.5, and 0.3, respectively. Many subsequent missions have confirmed these peaks and mapped other higher multipoles of the temperature and polarization fluctuations of the CMBR. These measurements are considered essential to cosmological models. The standard model is a piecemeal set of inferences about the evolution of the cosmos. First, there is an inflation piece wherein a random infinitesimally small region of an infinitesimally small Universe of essentially infinite energy

density that for an unknown reason ballooned to relative gargantuan size instantaneously by an unknown mechanism, and stopped for some unknown reason. It remains inexplicable why inflation doesn't happen again at any point in the Universe. Gravity waves existed in whatever under went inflation, but it is inexplicable whether matter, energy, gravity, known forces, or the current properties of spacetime held in the inflation state to manifest the gravity waves. After inflation stopped, for an unknown reason, there was a Big Bang with gravity-driven acoustic standing wave oscillations of the fireball plasma. Everything was created in the Big Bang as whatever it was expanded. But, rather than slow down, the Universe was observed to be accelerating in its expansion. So, at some point, dark energy took over; even though, there is no evidence of the identity of dark energy, and its mechanism of causing the accelerated expansion is unknown. The rate of the acceleration caused by dark energy cannot be predicted by the model. Another challenge is that the amount of mass of the Universe that is observable is only a small percentage based on gravity effects of the predominantly unseen mass of the Universe. Thus, nonbaryonic dark matter—exotic unidentified matter that exerts a gravitational attraction but has essentially no other interaction observed for normal matter such as absorption of light, is added as another parameter in the models. Many adjustable parameters were invented to try to meld the inhomogeneous pieces into continuity of the creation, appearance, behavior, and fate of the Universe.

The fluctuations in the CMBR are believed to be key since they are attributed to signatures from the early pieces, inflation and Big Bang. Specifically, the CMBR peaks are incorporated into adiabatic inflationary cosmology models wherein the at least 10 parameters are fully adjustable to fit the data supposedly corresponding to gravity waves during inflation, gravity-driven acoustic oscillations in the primordial plasma, and nonbaryonic dark matter. Yet, there is no guarantee that these occurred or that the CMBR is such a signature. There are many variants of the four-piece standard theory that are no more than models comprising conjectures about the state and occurrences of the early Universe. The four principle conjectures are not based on physical laws or mechanisms. Inflation occurred at infinitely faster than light speed that defies the laws of wave propagation of any kind. But, consider the gravity waves of inflation with the conjecture that the laws of gravity existed under the conditions of infinite energy density of unknown composition expanding at an near infinite rate as proposed. As given in the Absolute Space Confirmed Experimentally section, there is no physical basis for a transverse light-speed propagating gravity field to comprise a gravity wave consistent with the absence of the direct experimental observation of gravity waves [118,119]. Next, consider the gravity-driven acoustic oscillations in the primordial Big Bang plasma. Acoustic waves are not observed in plasmas, and if the Sun were analogous to the primordial plasma, helioseismology data shows no resemblance to orderly spherical harmonic waves [120]. Such acoustic waves in plasma, if they could exist, could not seed the structure of the Universe since acoustic waves would have a propagation velocity far less than the speed of light. Acoustic waves would be perturbed by plasma instabilities due to electromagnetic forces that dominate plasma physics. Furthermore, standing waves are precluded in rapidly expanding plasma. Consider that these inflationary models require the assignment of dark matter, which is essentially all of the matter in the Universe, as exotic nonbaryonic matter. The identity of dark matter has been a cosmological mystery. Postulated assignments include τ neutrinos, but a detailed search for signature emissions has yielded nil [121]. The search for signatures by the Cryogenic Dark Matter Search (CDMS) developed to detect theorized Weakly Interacting Massive Particles (WIMPs) has similarly yielded nil [122,123]. Moreover, detection of alternative hypothesized identities for

dark matter such as super-symmetry particles such as neutalinos has failed at the Large Hadron Collider; nor, has a single event been observed for weakly interacting massive particles or WIMPs at the Large Underground Xenon (LUX) experiment [99]. WIMP theory's main competitor known as MACHO theory assigns the Dark Matter to Massive Compact Halo Objects (MACHOs) which rather than elusive subatomic particles comprises ordinary baryonic matter in the form of burned-out dark stars, stray planets, and other large, heavy, but dark objects that must be ubiquitous throughout the Universe. However, MACHO theory has also recently been ruled out based on lack of evidence of these dark objects observable by the brief ellipses caused by them moving in front of distant stars. Only a few such objects have been observed after exhaustively searching for over five years [122,123].

As given in the Disproportionation of Energy States section, since the potential energy of atomic hydrogen is 27.2 eV, $m\ H$ atoms serve as a catalyst of $m \cdot 27.2\ eV$ for another $(m+1)$th H atom to form hydrino to H(1/(m +1)). For example, a H atom can act as a catalyst for another H by accepting 27.2 eV from it via through-space energy transfer such as by magnetic or induced electric dipole-dipole coupling to form an intermediate that decays with the emission of continuum bands with short wavelength cutoffs and energies of $m^2 \cdot 13.6\ eV$ $\left(\frac{91.2}{m^2}\ nm\right)$. The recording of high-energy continuum radiation from hydrogen as it forms hydrinos in the laboratory [59-64] has astrophysical implications such as hydrino being a candidate for the identity of dark matter and the corresponding emission being the source of high-energy celestial and stellar continuum radiation [59-64,65,66]. $m\ H$ catalyst (Eqs. (5.48-5.61)) was shown to be active in astronomical sources [59]. Hydrogen continua from transitions to form hydrinos provides a possible mechanism of linking the temperature and density conditions of the different discrete layers of the coronal/chromospheric sources. EUV spectra of white dwarfs matches the continua for H(1/2), H(1/3), and H(1/4), and the 10.1 nm continuum is observed from interstellar medium. The hydrino continuum radiation matches the diffuse ubiquitous EUV and soft X-ray cosmic background [79,81] with the 10.1 nm continuum matching the observed intense 11.0-16.0 nm band, the radiation source behind the observation that diffuse Hα emission is ubiquitous throughout the Galaxy and widespread sources of flux shortward of 912 $\AA$ are required [79], and the source of ionization of the interstellar medium (ISM) wherein a large component of the baryonic matter of the Universe is in the form of WHIM (warm-hot ionized media) in the absence of a conventional source [82,83,85]. Moreover, recent X-ray absorption data reveals that the temperature of galactic halo gas is in the range of 86 eV to 215 eV which is in the realm of the energy released for the transition of H to H(1/4) [85]. Indirect emission from ions of nonthermal origin is a feature of the continuum radiation emitted from hydrino transitions in celestial sources as well as hydrogen pinch plasmas at oxidized electrodes and solid fuel plasmas in the laboratory [59].

Hydrogen is known to comprise about 95% of the visible matter of the Universe. Recently, the missing mass has been showed to be baryonic rather than strange matter [45] (See Composition of the Universe section). Astrophysical [86,87,96,98] and direct laboratory spectroscopic data [59-64] indicate that the dark matter is also hydrogen, but in a lower-energy state. Thus, it comprises ordinary baryonic matter. Hydrogen atoms in these states exert a gravitational force, but do not resonantly absorb photons. Lower-energy atomic hydrogen atoms, hydrinos, each have the same mass and a similar interaction as the neutron. According to Steinhardt and Spergel of Princeton University [72], these are the properties of dark matter that are necessary in order for the theory of the structure of galaxies to work out on all scales. Rather

than curve fitting the peaks corresponding to the anisotropy in the CMBR, the data is predicted due to the time harmonic oscillation of the Universe due to the relationship between energy-matter (matter-energy) conversion and spacetime contraction (expansion) without requiring that the Universe is almost entirely comprised of exotic unidentified matter. A classical, closed-form solution of the CMBR using physical laws provides a rational alternative explanation to inflation-Big Bang-dark energy-exotic nonbaryonic dark matter cosmology.

When the Universe reaches the maximum radius corresponding to the maximum contribution of the amplitude, $\aleph_o$, of the time harmonic variation in the radius of the Universe, (Eq. (32.150)), it is entirely radiation-filled. Since the photon has no gravitational mass, the radiation is uniform. As energy converts into matter the power of the Universe may be considered negative for the first quarter cycle starting from the point of maximum expansion as given by Eq. (32.161), and spacetime contracts according to Eq. (32.140). The gravitational field from particle production travels as a light wave front. As the Universe contracts to a minimum radius, the gravitational radius given by Eq. (32.147), constructive interference of the gravitational fields occurs. The resulting slight variations in the density of matter are observed from our present r-sphere. The observed radius of expansion is equivalent to the radius of the light sphere with an origin at the time point when the Universe stopped contracting and started to expand.

Consider the effect of the expansion and contraction of the Universe on the unperturbed condition of uniform energy-matter density and a static Universe. The radius of the Universe time and spatially oscillates wherein the radius as a function of time is given by Eqs. (32.153) and (32.184). The Universe is a 3-sphere hyperspace of constant positive curvature that expands and contracts cyclically in all directions relative to an embedded space-time observer at his r-sphere. The harmonic oscillation of the radius of the Universe and thus its volume gives rise to delays and advances to light spheres of the continuum of r-spheres of the Universe that would otherwise propagate at relative velocity c. The gravitational field from particle production travels as a light wave front. As the radius of the Universe changes constructive interference of the gravitational fields occurs as the distance between r-spheres changes such that the fronts are advanced or delayed to interfere with each other. The resulting slight variations in the density of matter are observed from our present r-sphere. These variations would be observed as spherical harmonics corresponding to the spherical contraction and expansion in all directions. For each r-sphere, the angular variation in density corresponds to an angular distribution of the power of the Universe (Eq. (32.161)) and thus the temperature of the Universe according to the Stefan-Boltzmann law (Eq. (32.168)). These angular harmonic temperature variations are predominantly unpolarized, but posses a slight E-mode polarization and a lesser and B-mode polarization (Figure 32.13).

Figure 32.13. Color scale temperature variations and temperature variations of the E-mode and B-mode polarization of the CMBR of the Universe in degrees μK. Courtesy of NASA, G. Hinshaw, *et al*.

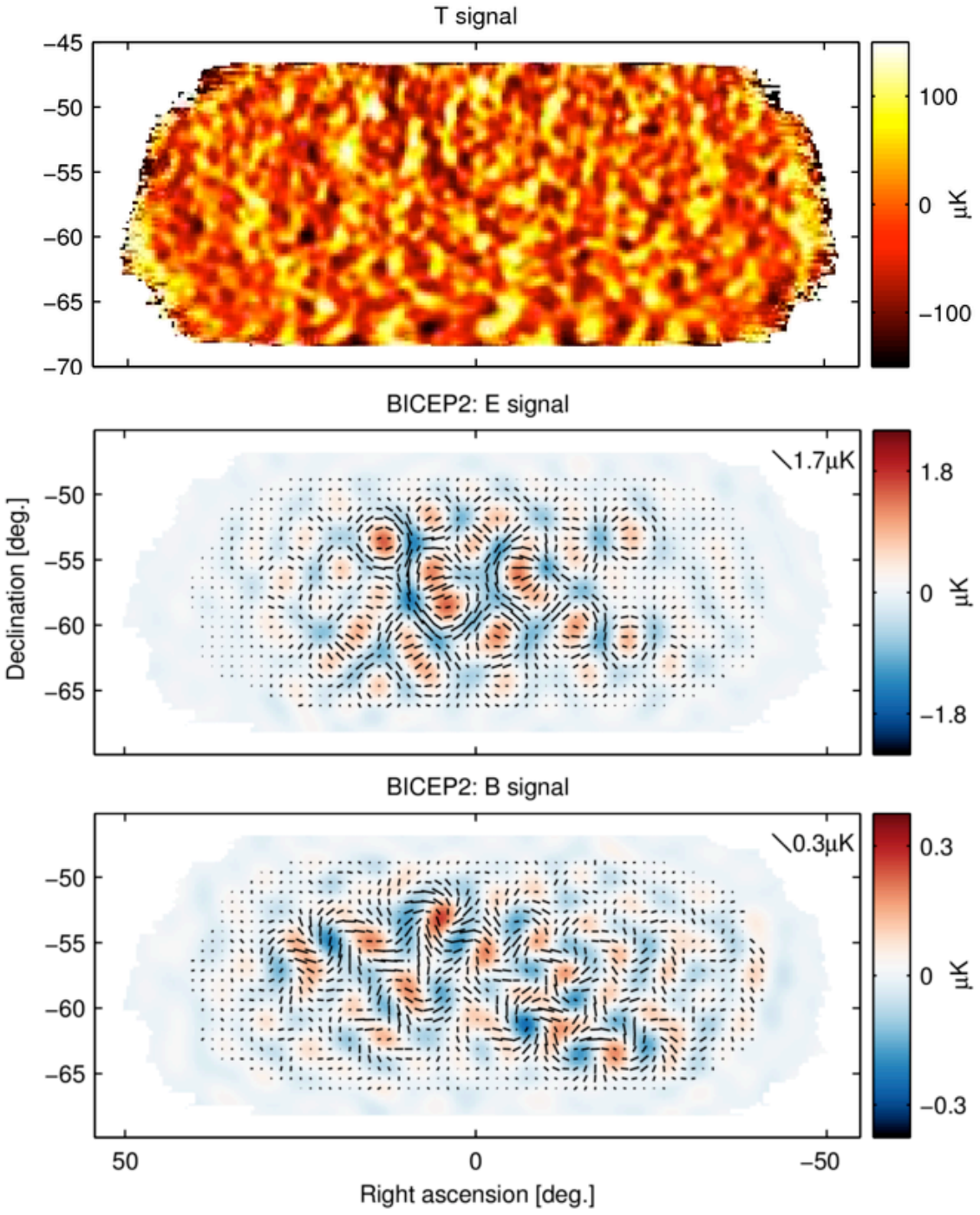

The angular variation in temperature is given by the Fourier transform of the observer's r-sphere temperature over the oscillatory period starting at matter formation at the initial time of

contraction through the initiation of expansion to the present time in the expansion cycle. The temperature of the Universe at each r-sphere $T_U(t)$ as a function of time is given by Eq. (32.168). The present r-sphere corresponds to a radial delta function ($f(r) = \frac{1}{r_{sphere}^2}\delta(r - r_{sphere})$) having the radius r_{sphere}. The temperature variation ΔT given by the spacetime Fourier transform of $T_U(t)$ in three dimensions in spherical coordinates plus time is given [124,125] as follows:

$$\Delta T(s,\Theta,\Phi,\omega) =$$

$$\int_0^\infty \int_0^{2\pi} \int_0^\pi \int_0^\infty \left[T_U(t)\frac{1}{r_{sphere}^2}\delta(r - r_{sphere}) \exp\left(-i2\pi sr[\cos\Theta\cos\theta + \sin\Theta\sin\theta\cos(\phi - \Phi)]\right)\exp(-i\omega t)\right] r^2 \sin\theta\, dr\, d\theta\, d\phi\, dt \quad (32.190)$$

With spherical symmetry [124],

$$\Delta T(s,\omega) = 4\pi \int_0^\infty \int_0^\infty T_U(t)\frac{1}{r_{sphere}^2}\delta(r - r_{sphere})\text{sinc}(sr)r^2\exp(-i\omega t)\, dr\, dt \quad (32.191)$$

$$\Delta T(s,\omega) = 4\pi \int_0^\infty T_U(t)\text{sinc}(sr_{sphere})\exp(-i\omega t)\, dt$$

$$\Delta T(\ell,\omega) = 4\pi \int_0^\infty T_U(t)\text{sinc}\left(\frac{\pi}{140}\ell\right)\exp(-i\omega t)\, dt \quad (32.192)$$

where the Fourier wavenumber s is the multipole moment $\ell = \frac{2\pi}{\theta}$ due to the observable angular variations at the observer's (present) r-sphere due to radius, power, area, and temperature oscillations is all directions of the four-dimensional hyperspace of constant positive curvature. The corresponding angular multipole of the radius of the present expansion r-sphere after the half-period of contraction $\frac{\pi}{\ell_{sphere}}$ is substituted for r_{sphere}. The spherical harmonic parameter ℓ_{sphere} of the interference is given by the ratio of the amplitude, $\aleph_o$, of the time harmonic variation in the radius of the Universe, (Eq. (32.150)) divided by the observer's present r-sphere radius. The latter is given by the sum of ct (the light sphere due to light speed for $t = 10^{10}\ light\ years = 3.069\ X\ 10^3\ Mpc$) and the differential in the radius of the Universe $\Delta\aleph$ due to its acceleration is given by Eq. (32.189) wherein $\ddot{\aleph}$ is given by Eq. (32.155). As shown in Figure 32.11 the differential in the radius of the Universe $\Delta\aleph$ due to its acceleration is

$$\begin{aligned}\Delta\aleph &= 1/2\ddot{\aleph}t^2 \\ &= \frac{1}{2}\left(8.04\ X\ 10^{-11}\right)\cos\left(\frac{2\pi\left(1\ X\ 10^{10}\ yrs\right)}{9.83\ X\ 10^{11}\ yrs}\right)\ \frac{light\ years}{yrs^2}\left(1\ X\ 10^{10}\ yrs\right)^2 \\ &= 4.02\ X\ 10^9\ light\ years\end{aligned} \quad (32.193)$$

The radius r_{sphere} of the currently observed Universe is thus

$$\begin{aligned} r_{sphere} &= ct + \Delta\aleph \\ &= 10^{10}\ light\ years + 4.02\ X\ 10^{9}\ light\ years \\ &= 14.02\ X\ 10^{9}\ light\ years \end{aligned} \tag{32.194}$$

The angular scale or spherical harmonic parameter ℓ_{sphere} is

$$\ell_{sphere} = \frac{\aleph_0}{r_{sphere}} = \frac{\aleph_0}{ct + \Delta\aleph} = \frac{1.97\ X\ 10^{12}\ light\ years}{10^{10}\ light\ years + 4.02\ X\ 10^{9}\ light\ years} = 140 \tag{32.195}$$

$T_U(t)$ given by Eq. (32.168) is a complicated function of ratios of sums of constants and trigonometric equations to different exponents. However, from Figure 32.9, it can be appreciated that $T_U(t)$ during the contraction phase is represented to good approximation by the equation:

$$T_U(t) = \left(0.01 + 5.98\ X\ 10^{-12}\ yrs^{-1} t\right) K \tag{32.196}$$

Substitution of Eqs. (32.195) and (32.196) into Eq. (32.192) with the proper limits on the contraction time and considering the incremental solid angle gives

$$\Delta T(\ell,\omega) = \omega \int_{T/2}^{T} \left(0.01 + 5.98\ X\ 10^{-12}\ yrs^{-1} t\right) \mathrm{sinc}\left(\frac{\pi}{140}\ell\right) \exp(-i\omega t)\, dt\ K \tag{32.197}$$

$$\begin{aligned} \Delta T(\ell) &= \left(0.01 + \left(5.9\ X\ 10^{-12}\ yrs^{-1}\right)\left(\left(\frac{9.83\ X\ 10^{11}\ yrs}{2}\right)\right)\right) \mathrm{sinc}\left(\frac{\pi}{140}\ell\right) K \\ \Delta T(\ell) &= 3\,\mathrm{sinc}\left(\frac{\pi}{140}\ell\right) K \end{aligned} \tag{32.198}$$

The amplitude of the temperature fluctuations are dependent on the relative areas of the current r-sphere to that of the radius of the initiation of contraction. The scaling factor $C_{Tsphere}$ is given by

$$\begin{aligned} C_{Tsphere} &= \left(\frac{ct}{\aleph_0}\right)^{-2} = \left(\frac{ct}{\frac{m_U c}{Q}}\right)^{-2} = \left(\frac{t}{2T}\right)^{-2} \\ &= \left(\frac{ct}{\frac{2\ X\ 10^{54}\ kg}{\frac{c^3}{4\pi G}}}\right)^{-2} = \left(\frac{10^{10}\ light\ years}{1.97\ X\ 10^{12}\ light\ years}\right)^{-2} = \left(197\right)^{-2} \end{aligned} \tag{32.199}$$

Using Eq. (32.199), the correction of the temperature for the current r-sphere area relative to the maximum area gives

$$\Delta T(\ell) = C_{Tsphere}\, 3\,\mathrm{sinc}\left(\frac{\pi}{140}\ell\right) K = 77\,\mathrm{sinc}\left(\frac{\pi}{140}\ell\right) \mu K \tag{32.200}$$

The temperature variation is shifted by the relative position of the current light sphere with the

limiting one. Specifically, the ℓ_0 shift is given by the ratio of the amplitude, $\aleph_o$, of the time harmonic variation in the radius of the Universe (Eq. (32.150)), divided by the present radius of the light sphere, $ct = 10^{10}\ light\ years = 3.069\ X\ 10^3\ Mpc$. Using Eq. (32.199), the shift is given by

$$\ell_0 = \frac{\aleph_0}{ct} = \frac{\frac{m_U c}{Q}}{ct} = \frac{2T}{t} = \frac{\frac{2\ X\ 10^{54}\ kg}{\frac{c^3}{4\pi G}}}{ct} = \frac{1.97\ X\ 10^{12}\ light\ years}{10^{10}\ light\ years} = 197 \tag{32.201}$$

Substitution of the shift given by Eq. (32.201) into Eq. (32.200) gives the temperature variations in degrees μK as a function of multipole moment ℓ:

$$\Delta T(\ell) = 77 \text{sinc}\left(\frac{\pi}{140}\left(\ell - 197\right)\right) \mu K \tag{32.202}$$

for $\ell > 0$. A plot of Eq. (32.202) is given in Figure 32.14. The predictions match the DASI observed amplitude of $77 \mu K$ and the peaks at $\ell \approx 200$, $\ell \approx 550$, and $\ell \approx 800$ with relative intensities of 1, 0.5, and 0.3, respectively [35,126-129]. The plot of the corresponding power spectrum comprising spherical harmonic coefficient $\frac{\ell(\ell+1)C_\ell}{2\pi}\left[\mu K^2\right]$ amplitudes as a function of multipole ℓ is shown in Figure 32.15. The power spectrum plot is the square of Eq. (32.202) made positive-definite by first adding the corresponding constant to it before squaring. The amplitude was normalized to 77 μK squared. The experimental power spectrum of WMAP with the data of SPT and ACT [130], and best curve fit comprising spherical harmonic coefficient $\frac{\ell(\ell+1)C_\ell}{2\pi}\left[\mu K^2\right]$ amplitudes as a function of multipole ℓ for the temperature variations of the CMBR of the Universe is shown in Figure 32.16. There is excellent agreement between the predicted and experimental multipole temperature fluctuation curves.

Figure 32.14. The temperature variations and temperature variations of the E-mode and B-mode polarization of the CMBR of the Universe in degrees μK as a function of multipole moment ℓ.

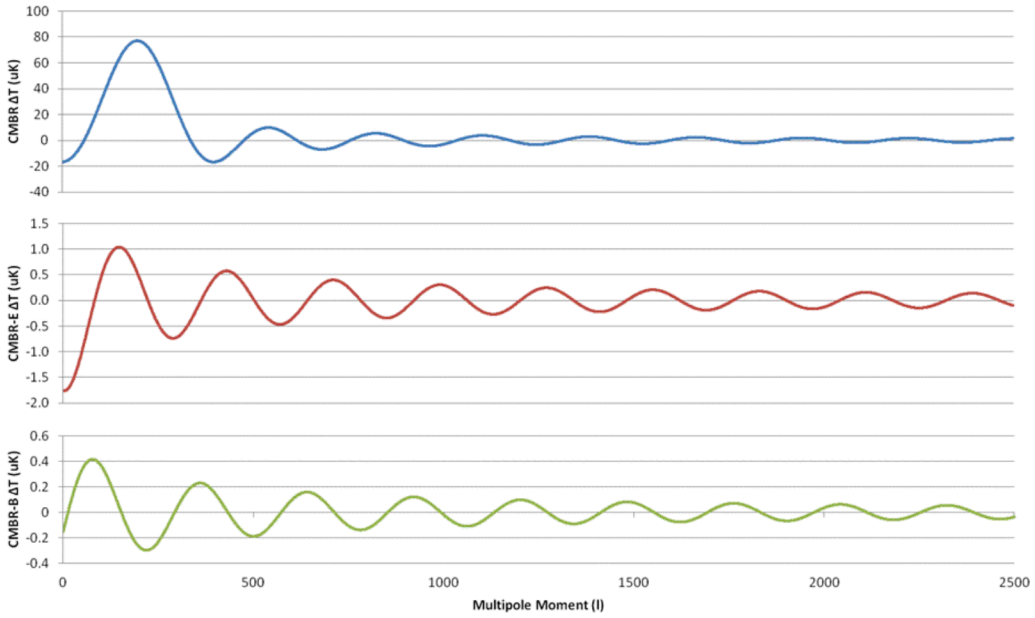

Figures 32.15A-B. The power spectrum comprising spherical harmonic coefficient $\frac{\ell(\ell+1)C_\ell}{2\pi}\left[\mu K^2\right]$ amplitudes as a function of multipole ℓ for the temperature variations and temperature variations of the E-mode and B-mode polarization of the CMBR of the Universe. The experimental data points of BICEP2 [131,132] for the E-mode peak at $\ell = 140$ and the B-mode peak at $\ell = 70$, $r = 0.20^{+0.07}_{-0.05}$ are superimposed. A. Plot over the range $0 \le \ell \le 2500$. B. Plot over the range $0 \le \ell \le 200$.

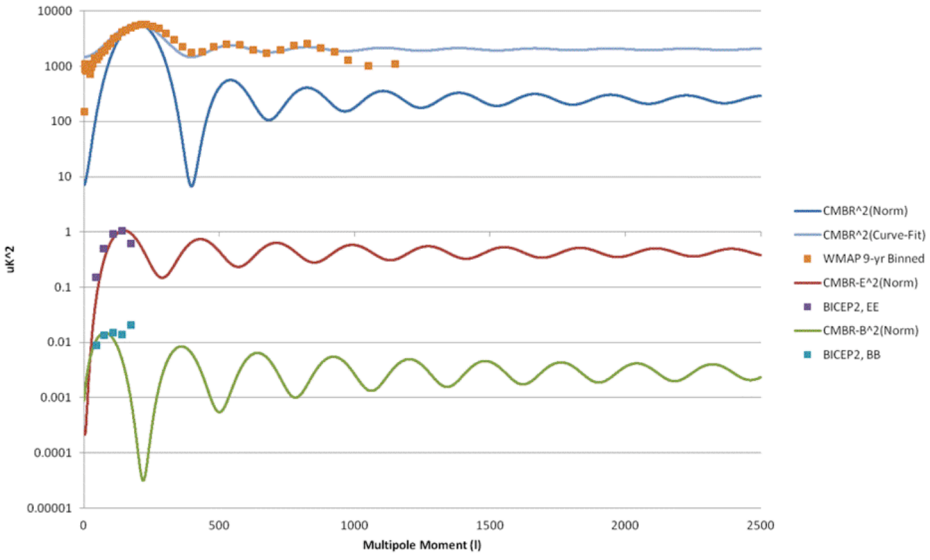

(A)

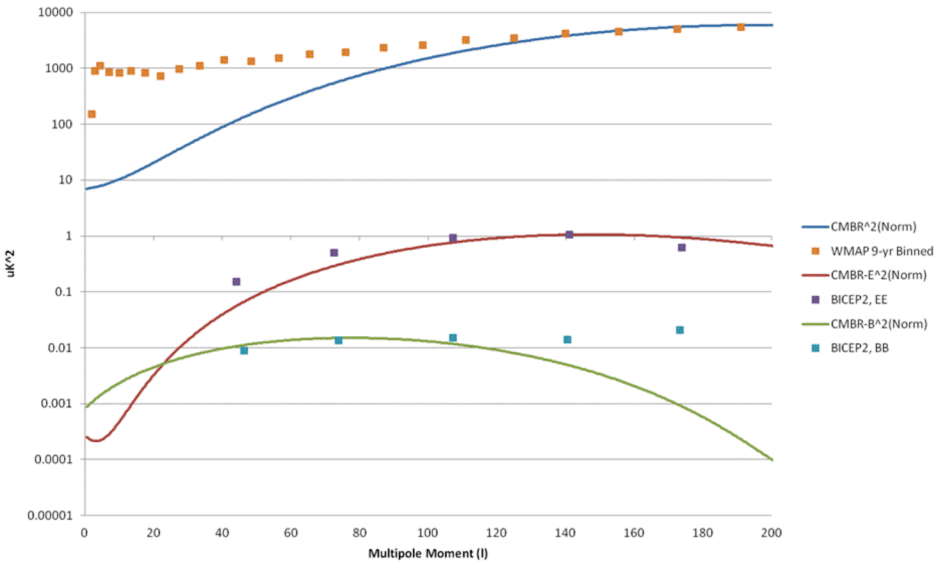

(B)

Figure 32.16. The experimental power spectrum of WMAP with the data of SPT and ACT [130] and best curve fit comprising spherical harmonic coefficient $\frac{\ell(\ell+1)C_\ell}{2\pi}\left[\mu K^2\right]$ amplitudes as a function of multipole ℓ for the temperature variations of the CMBR of the Universe. Courtesy of NASA, G. Hinshaw, *et al*.

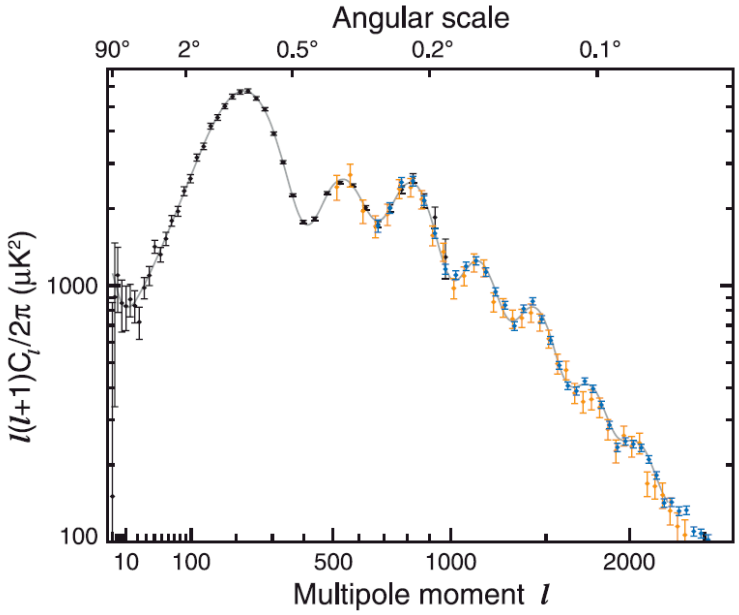

Polarized light is produced as correlation multipoles of the CMBR temperature fluctuations by Thompson scattering of the CMBR by stellar and interstellar medium plasma electrons (essentially ionized hydrogen) over the half period of contraction $T_U / 2 = 4.92\ X\ 10^{11}$ *years* plus the time of expansion $t = 10^{10}$ *years*. The phase shift corresponds to an opposite sign of the shift of Eq. (32.202), an advance in the cosmic microwave

background radiation temperature modulation rather than a delay:

$$\Delta T_{\text{E-mode}}(\ell) = C_{\text{effThompson}} 77 \text{sinc}\left(\frac{\pi}{140}\left(\ell + 197\right) \right) \mu K \tag{32.203}$$

wherein $\ell > 0$ and C_{eff} is the Thompson polarization constant that is a small fraction corresponding to the weakness of Thompson scattering. The constant may be calculated from the temperature fluctuations, the blackbody electromagnetic radiation spectrum, and the plasma density of the Universe over the cycle from the commencement of contraction to the present r-sphere. The first peak is predicted at $\ell = 140$ which matches that observed by BICEP2 [131,132].

The polarization pattern of the Thompson scattered CMBR comprises a curl free component call E-mode since it is electric-field-like or gradient-mode with no handedness. Gravitational lensing causes E-mode polarization to convert to a gradient free component call B-mode since it is magnetic-field-like or curl-mode with handedness. Another mechanism to achieve polarized B-mode angular variations in the CMBR is based on the acceleration of the expansion of spacetime. The Universe is matter-filled at the transition time point from contraction to expansion. Thus, the light sphere propagates into a Universe that is much older and larger according to Eq. (32.153) with time equal to the elapsed time from the commencement of expansion. The light sphere expands at light speed, but into spacetime that is accelerating in its expansion. Due to the acceleration of the light-speed propagating light sphere, E-mode light experiences the same spacetime gradients as in the case of gravitational lensing; consequently, E-mode is converted to B-mode polarization. The B-mode radiation is shifted by $\frac{\pi}{2}$ relative to the E-mode radiation. Thus, Eq. (32.203) gives the B-mode radiation pattern as

$$\Delta T_{\text{B-mode}}(\ell) = r^{1/2} C_{\text{effThompson}} 77 \text{sinc}\left(\frac{\pi}{140}\left(\ell + 197 + 70\right) \right) \mu K \tag{32.204}$$

for $\ell > 0$. The first peak is predicted at $\ell = 70$. The E-mode polarized radiation should be substantially less intense than fluctuations in the CMBR since it is Thompson scattered radiation. Furthermore, the B-mode radiation should been a fraction of the E-mode since the latter is converted from the former. Consider that the mode conversion by accelerating spacetime is limited by the relative extent of the acceleration. The ratio $r^{1/2}$ of the amplitude ΔT of the B-mode to E-mode components is given by the ratio of the differential radius due to acceleration $\Delta\aleph$ and the radius due to light sphere expansion ct. Thus, using Eq. (32.193), the ratio $r^{1/2} = \frac{\Delta T\left(\text{B-mode}\right)}{\Delta T\left(E\text{-mode}\right)}$ is

$$r^{1/2} = \frac{\Delta T\left(B\text{ - mode}\right)}{\Delta T\left(E\text{ - mode}\right)} = \frac{\Delta\aleph}{\left(ct\right)} = \left(\frac{4.02\ X\ 10^{9}\ \ light\ years}{10^{10}\ \ light\ years} \right) = 0.40 \tag{32.205}$$

The ratio r of the amplitude ΔT^2 of the B-mode to E-mode power spectral components is

$$r = \left[\frac{\Delta T\left(B\text{ - mode}\right)}{\Delta T\left(E\text{ - mode}\right)} \right]^2 = 0.16 \tag{32.206}$$

Substitution of Eq. (32.206) into Eq. (32.204) gives

$$\Delta T_{\text{B-mode}}(\ell) = C_{\text{effThompson}}\, 31 \text{sinc}\left(\frac{\pi}{140}\left(\ell + 197 + 70\right)\right)\ \mu K \tag{32.207}$$

BICEP2 [132] reports a value of $r = 0.20^{+0.07}_{-0.05}$ $\ell = 70$ that is in good agreement with predictions. The plots of the corresponding E-mode and B-mode power spectra comprising spherical harmonic coefficient $\frac{\ell(\ell+1)C_\ell}{2\pi}\left[\mu K^2\right]$ amplitudes as a function of multipole ℓ are shown in Figure 32.15. The E-mode and B-mode power spectral plots are the square of Eqs. (32.203) and (32.207), respectively, each made positive-definite by first adding the corresponding constant to it before squaring. Each plot was normalized by the corresponding squared amplitude of the ΔT plot. $C_{\text{effThompson}}$ can be calculated, but for convenience it was taken as the experimental ratio of $\Delta T_{\text{E-mode}}(\ell)$ to $\Delta T(\ell)$. The BICEP2 [132] experimental data points for the E-mode peak at $\ell = 140$ and the B-mode peak at $\ell = 70$ are shown. There is excellent agreement between the predicted and experimental multipole polarization temperature fluctuation curves.

The definitive form of the field equations of general relativity follow from the Schwarzschild metric (Eq. (32.38)) and can be expressed in terms of ***the contraction of spacetime by the special relativistic mass of a fundamental particle*** (Eq. (32.140)). The masses and charges of the fundamental particles are determined by the equations of the transition state orbitsphere herein derived where the nonradiative boundary condition and the constancy of the speed of light must hold which requires relativistic corrections to spacetime. Fundamental particles can decay or interact to form an energy minimum. Thus, each stable particle arises from a photon directly or from a decaying particle, which arose from a photon. The photon, and the corresponding fundamental particle, possess $\hbar$ of angular momentum. Nuclei form as binding energy is released as the orbitspheres of participating nucleons overlap. Atoms form as the potential energy of the fields of electrons and nuclei is released as the fields are partially annihilated. Molecules form as the energy stored in the fields of atoms is minimized. Planets and celestial bodies form as the gravitational potential energy is minimized. All of these energies correspond to forces, and the equations of the forces are given in the Unification of Spacetime, the Forces, Matter, and Energy section.

REFERENCES

1. E. G. Adelberger, C. W. Stubbs, B. R. Heckel, Y. Su, H. E. Swanson, G. Smith, J. H. Gundlach, Phys. Rev. D, Vol. 42, No. 10, (1990), pp. 3267-3292.
2. H. Minkowski's interpretation of special relativity in terms of a four dimensional space time was presented in the form of a lecture in Cologne, Germany in September 1908. An English translation, entitled "Space and Time," can be found in the collection *The Principle of Relativity*, Dover, New York, 1952.
3. V. Fock, *The Theory of Space, Time, and Gravitation*, The MacMillan Company, (1964), pp. 14-15.
4. E. Giannetto, The rise of special relativity: Henri Poincaré's works before Einstein. Atti del 18 Congresso di Storia della Fisica e dell'Astronomia, (1998), pp. 171-207, [http://www.brera.unimi.it/old/Atti-Como-98/Giannetto.pdf].
5. H. Poincaré, "L'etat actuel et l'avenir de la physique mathematique," *Bulletin des sciences mathematiques*, Vol. 28, (1904), pp.302-324; quoted in Whittaker (1987), p. 30.
6. E. Whittaker, *A History of the Theories of Aether and Electricity*, Vol. 2, Modern Theories,

Chapter 2, "The Relativity Theories of Poincaré and Lorentz," Nelson, London, (1987), Reprinted, American Institute of Physics, pp. 30–31.
7. E. Fomalont, S. Kopeikin, "How fast is gravity," New Scientist, Vol. 177, Issue 2377, Jan. 11, (2003), pp. 32.
8. L. Z. Fang, and R. *Ruffini, Basic Concepts in Relativistic Astrophysics*, World Scientific, (1983).
9. A. Beiser, *Concepts of Modern Physics*, Fourth Edition, McGraw-Hill Book Company, New York, (1978), pp. 88-89.
10. G. R. Fowles, *Analytical Mechanics*, Third Edition, Holt, Rinehart, and Winston, New York, (1977), pp. 154-155.
11. V. Fock, *The Theory of Space, Time, and Gravitation*, The MacMillan Company, (1964).
12. W. K. Clifford, *The Common Sense of the Exact Sciences*, Mathematical Papers, p. 21, presented to the Cambridge Philosophical Society in 1870.
13. R. M. Wald, *General Relativity*, University of Chicago Press, Chicago, (1984), pp. 91-101.
14. N. A. Bahcall, J. P. Ostriker, S. Perlmutter, P. J. Steinhardt, Science, May 28, 1999, Vol. 284, pp. 1481-1488.
15. R. Lieu, L. W. Hillman, "The phase coherence of light from extragalactic sources—direct evidence against first order Planck scale fluctuations in time and space," Astrophysical Journal Letters, March 10, (2003).
16. R. Ragazzoni, M. Turatto, W. Gaessler, "The lack of evidence for quantum structure of spacetime at Planck scales," Astrophysical Journal, April 10, (2003), Vol. 587, L1-L4.
17. V. Fock, *The Theory of Space, Time, and Gravitation*, The MacMillan Company, (1964), pp. 209-215.
18. S. Weinberg, *Gravitation and Cosmology: Principles and Applications of the General Theory of Relativity*, John Wiley & Sons, New York, (1972), Sect. 11/7, pp. 335 ff.
19. L. P. Eisenhart, *Riemannian Geometry*, Princeton: Princeton University Press, (1949).
20. D. Lovelock, "The Four Dimensionality of Space and the Einstein Tensor," J. Math. Phys., Vol. 13, (1972), pp. 874-876.
21. R. M. Wald, *General Relativity*, University of Chicago Press, Chicago, (1984), Chp. 9 and Chp. 14.
22. A. Linde, "The Self Reproducing Inflationary Universe," Scientific American Presents, Spring (1998), Vol. 9 pp. 98-104.
23. I. Levine, *Physical Chemistry*, McGraw-Hill Book Company, (1978).
24. T. Gold, Am. J. Phys., 30, 403 (1962).
25. R. S. Casella, Phys. Rev. Lett., 21, 1128 (1968).
26. R. S. Casella, Phys. Rev. Lett., 22, 554 (1969).
27. Y. Ne'eman, Int. J. Theoret. Phys., 3, 1 (1970).
28. W. L. Freeman, et. al., Nature, 371, pp. 757-762, (1994).
29. W. L. Freeman et. al., "Final Results from the Hubble Space Telescope Key Project to measure the Hubble constant," Astrophysical Journal, Vol. 553, May 20, (2001), pp. 47-72.
30. R. F. Mushotzky, Meeting of the American Astronomical Society, Phoenix, AZ, (January 4, 1994).
31. D. N. Schramm, Physics Today, April, (1983), pp. 27-33.
32. S. W. Hawking, *A Brief History of Time*, Bantam Books, Toronto, (1988), p. 11.
33. J. C. Mather, et. al., The Astrophysical Journal, 354, L37-L40, (1990).

34. A. Beiser, *Concepts of Modern Physics*, Fourth Edition, McGraw-Hill Book Company, New York, (1978), pp. 329-339.
35. N. W. Halverson, E. M. Leitch, C. Pryke, J. Kovac, J. E. Carlstrom, W. L. Holzapfel, M. Dragovan, J. K. Cartwright, B. S. Mason, S. Padin, T. J. Pearson, M. C. Shepard, and A. C. S. Readhead, "DASI first results: a measurement of the cosmic microwave background angular power spectrum," arXiv:astro-ph/0104489, 30 April, (2001).
36. R. Lieu, J. P. D. Mittaz, S-N Zhang, "The Sunyaev-zel'dovich effect in a sample of 31 clusters: a comparison between the X-ray predicted and WMAP observed cosmic microwave background temperature decrement," The Astrophysical Journal, Vol. 648, (2006), pp. 176-199.
37. Science, Vol. 279, Feb., (1998), pp. 1298-1299.
38. Science News, Vol. 153, May, (1998), p. 344.
39. Science News, Vol. 154, October 31, (1998), p. 277.
40. R. M. Wald, *General Relativity*, University of Chicago Press, Chicago, (1984), pp. 114-116.
41. P. J. E. Peebles, J. Silk, Nature, Vol. 346, July, 19, (1990), p. 233-239.
42. Personal communication, Dr.-Ing. Günther Landvogt, Hamburg, Germany, January, (2003).
43. M. Davis, et. al., Nature, 356, (1992), pp. 489-493.
44. K. A. Olive, D. N. Schramm, G. Steigman, and T. P. Walker, Phys. Lett., B236, (1990), pp. 454-460.
45. F. Nicastro, A. Zezas, M. Elvis, S. Mathur, F. Fiore, C. Cecchi-Pestellini, D. Burke, J. Drake, P. Casella, "The far-ultraviolet signature of the 'missing' baryons in the local group of galaxies," Nature, Vol. 421, No. 13, pp. 719-721.
46. D. Stern, H. Spinrad, P. Eisenhardt, A. J. Bunker, S. Dawson, S. A. Stanford, R. Elston, "Discovery of a color-selected quasar at $z = 5.5$," Astrophysical Journal, Vol. 533, April 20, (2000), pp. L75-L78.
47. X. Fan, et al., "A survey of $z > 5.8$ quasars in the Sloan Digital Sky Survey I: discovery of three new quasars and the spatial density of luminous quasars at $z \approx 6$," Astrophysical Journal, December, (2001).
48. CERN Courier, June, (1996), p. 1.
49. L. Farrarese, D. Merritt, Astrophysical Journal, Vol. 539, (2000) p. L9.
50. K. Gebhardt, et al., Astrophysical Journal, Vol. 539, (2000) p. L13.
51. S. Flamsteed, Discover, Vol. 16, Number 3, March, (1995), pp. 66-77.
52. J. Glanz, Science, Vol. 273, (1996), p. 581.
53. http://www.eurekalert.org/pub_releases/2004-01/ci-ogi010504.php.
54. http://www.eurekalert.org/pub_releases/2004-01/nsf-ase010804.php.
55. http://www.gemini.edu/gdds/.
56. K. Glazebrook, R. G. Abraham, P. J. McCarthy, S. Savaglio, H-W Chen , D. Crampton, R. Murowinski, I. Jorgensen, K. Roth, I. Hook, R. O. Marzke, R. G. Carlberg, "A high abundance of massive galaxies 3-6 billion years after the Big Bang," Nature, Vol. 430, (2004) pp. 181-184.
57. A. Cimatti, E. Daddi, A. Renzini, P. Cassata, E. Vanzella, L. Pozzetti, S. Cristiani, A. Fontana, G. Rodighiero, M. Mignoli, G. Zamorani, "Old galaxies in the young Universe," Nature, Vol. 430, (2004), pp. 184-187.
58. D. Stark, R. S. Ellis, J. Richard, J-P. Kneib, G. P. Smith, M. R. Santos, "A Keck survey for gravitationally lensed Lyα emitters in the redshift range 8.5 < z < 10.4: New constraints on

the contribution of low-luminosity sources to cosmic reionization," The Astrophysical Journal, Vol. 663, No. 10, (2007), pp. 10-28.
59. R. Mills, Y. Lu, "Mechanism of soft X-ray continuum radiation from low-energy pinch discharges of hydrogen and ultra-low field ignition of solid fuels," submitted.
60. R. L. Mills, R. Booker, Y. Lu, "Soft X-ray Continuum Radiation from Low-Energy Pinch Discharges of Hydrogen," J. Plasma Physics, Vol. 79, (2013), pp 489-507; doi: 10.1017/S0022377812001109.
61. R. L. Mills, Y. Lu, "Time-resolved hydrino continuum transitions with cutoffs at 22.8 nm and 10.1 nm," Eur. Phys. J. D, Vol. 64, (2011), pp. 65, DOI: 10.1140/epjd/e2011-20246-5.
62. R. L. Mills, Y. Lu, "Hydrino continuum transitions with cutoffs at 22.8 nm and 10.1 nm," Int. J. Hydrogen Energy, 35 (2010), pp. 8446-8456, doi: 10.1016/j.ijhydene.2010.05.098.
63. R. L. Mills, Y. Lu, K. Akhtar, "Spectroscopic observation of helium-ion- and hydrogen-catalyzed hydrino transitions," Cent. Eur. J. Phys., 8 (2010), pp. 318-339, doi: 10.2478/s11534-009-0106-9.
64. A. Bykanov, "Validation of the observation of soft X-ray continuum radiation from low energy pinch discharges in the presence of molecular hydrogen," http://www.blacklightpower.com/wp-content/uploads/pdf/GEN3_Harvard.pdf.
65. M. A. Barstow and J. B. Holberg, *Extreme Ultraviolet Astronomy*, Cambridge Astrophysics Series 37, Cambridge University Press, Cambridge, (2003).
66. R. Stern, S. Bowyer, "Apollo-Soyuz survey of the extreme-ultraviolet/soft X-ray background", Astrophys. J., Vol. 230, (1979), pp. 755-767.
67. W. Sanders, et. al. Nature, 349, (1991), pp. 32-38.
68. R. P. Kirshner, A. J. Oemler, P. L. Schecter, and A. S. Schectman, AJ, (1983), 88,1285.
69. V. de Lapparent, V., M. J. Geller, and J. P. Huchra, ApJ, (1988), 332, 44.
70. A. Dressler, et. al., (1987), Ap. J., 313, L37.
71. S. A. Thomas, F. B. Abdalla, O. Lahav, "Excess clustering on large scales in the MegaZ DR7 Photometric Redshift Survey", Physical Review Letters, Vol. 106, (2011), pp. 241301-1-24310-4.
72. G. Musser, Scientific American, May, (2000), p. 24.
73. M. A. Barstow and J. B. Holberg, *Extreme Ultraviolet Astronomy*, Cambridge Astrophysics Series 37, Cambridge University Press, Cambridge, (2003), Chp 8.
74. M. Stix, *The Sun*, Springer-Verlag, Berlin, (1991), Figure 9.5, p. 321.
75. Phillips, J. H., *Guide to the Sun*, Cambridge University Press, Cambridge, Great Britain, (1992), pp. 126-127.
76. M. Stix, *The Sun*, Springer-Verlag, Berlin, (1991), pp. 351-356.
77. http://nobelprize.org/nobel_prizes/physics/articles/bahcall/.
78. N. Craig, M. Abbott, D. Finley, H. Jessop, S. B. Howell, M. Mathioudakis, J. Sommers, J. V. Vallerga, R. F. Malina, "The Extreme Ultraviolet Explorer stellar spectral atlas", The Astrophysical Journal Supplement Series, Vol. 113, (1997), pp. 131-193.
79. S. Labov, S. Bowyer, "Spectral observations of the extreme ultraviolet background", The Astrophysical Journal, 371, (1991), pp. 810-819.
80. A. F. H. van Gessel, Masters Thesis: *EUV spectroscopy of hydrogen plasmas*, April (2009), Eindhoven University of Technology, Department of Applied Physics, Group of Elementary Processes in Gas Discharges, EPG 09-02, pp. 61-70.
81. S. Bower, G. Field, and J. Mack, "Detection of an anisotrophic soft X-ray background flux," Nature, Vol. 217, (1968), p. 32.

82. C. W. Danforth, J. M. Shull, "The low-z intergalactic medium. III. H I and metal absorbers at z<0.4", The Astrophysical Journal, Vol. 679, (2008), pp. 194-219.
83. N. Werner, A. Finoguenov, J. S. Kaastra, A. Simionescu, J. P. Dietrich, J Vink, H. Böhringer, "Detection of hot gas in the filament connecting the clusters of galaxies Abell 222 and Abell 223", Astronomy & Astrophysics Letters, Vol. 482, (2008), pp. L29-L33.
84. S. Bowyer, J. J. Drake, S. Vennes, "Extreme ultraviolet spectroscopy", Ann. Rev. Astron. Astrophys., Vol. 38, (2000), pp. 231-288.
85. A. Gupta, S. Mathur, Y. Krongold, F. Nicastro, M. Galeazzi, "A huge reservoir of ionized gas around the Milky Way: Accounting for the missing mass?" The Astrophysical Journal Letters, Volume 756, Number 1, (2012), P. L8, doi:10.1088/2041-8205/756/1/L8.
86. F. Bournaud, P. A. Duc, E. Brinks, M. Boquien, P. Amram, U. Lisenfeld, B. Koribalski, F. Walter, V. Charmandaris, "Missing mass in collisional debris from galaxies", Science, Vol. 316, (2007), pp. 1166–1169.
87. B. G. Elmegreen, "Dark matter in galactic collisional debris", Science, Vol. 316, (2007), pp. 32-33.
88. P. Jean, et al., "Early SPI/INTEGRAL measurements of 511 keV line emission from the 4th quadrant of the Galaxy", Astron, Astrophys., Vol. 407, (2003), pp. L55-L58.
89. M. Chown, "Astronomers claim dark matter breakthrough," NewScientist.com, Oct. 3, (2003), http://www.newscientist.com/ article/dn4214-astronomers-claim-dark-matter-breakthrough.html.
90. C. Boehm, D. Hooper, J. Silk, M. Casse, J. Paul, "MeV dark matter: Has it been detected," Phys. Rev. Lett., Vol. 92, (2004), p. 101301.
91. G. H. Share, "Recent results on celestial gamma radiation from SMM", Advances in Space Research, Vol.11, Issue 8, (1991), pp. 85-94.
92. G. H. Share, R. L. Kinzer, D. C. Messina, W. R. Purcell, E. L. Chupp, D. J. Forrest, E. Rieger, "Observations of galactic gamma-radiation with the SMM spectrometer", Advances in Space Research, Vol. 6, Issue 4, (1986), pp. 145-148.
93. B. Kozlovsky, R. E. Lingenfelter, R. Ramaty, "Positrons from accelerated particle interactions," The Astrophysical Journal, Vol. 316, (1987), pp. 801-818.
94. E. P. Mazets, S. V. Golenetskii, V. N. Il'inskii, R. L. Aptekar', Y. A. Guryan, "Observations of a flaring X-ray pulsar in Dorado," Nature, Vol. 282, No. 5739, (1979), pp. 587-589.
95. G. H. Share, E. L. Chupp, D. J. Forrest, E. Rieger in *Positron and Electron Pairs in Astrophysics*, ed. M. L. Burns, A. K. Harding, R. Ramaty, "Positron annihilation radiation from Solar flares", (1983), New York: AIP, pp. 15-20.
96. M. J. Jee, et al., "Discovery of a ringlike dark matter structure in the core of the galaxy cluster C1 0024+17," Astrophysical Journal, Vol. 661, (2007), pp. 728-749.
97. R. L. Mills, *The Grand Unified Theory of Classical Quantum Mechanics*, November 1995 Edition, HydroCatalysis Power Corp., Malvern, PA, Library of Congress Catalog Number 94-077780, ISBN number ISBN 0-9635171-1-2, Chp. 22.
98. M. J. Jee, A. Mahdavi, H. Hoekstra, A. Babul, J. J. Dalcanton, P. Carroll, P. Capak, "A study of the dark core in A520 with the Hubble Space Telescope: The mystery deepens," Astrophys. J., Vol. 747, No.96, (2012), pp. 96-103.
99. D. S. Akerib, et al., "First results from the LUX dark matter experiment at the Stanford Underground Research Facility", (2014), http://arxiv.org/abs/1310.8214.
100. Hurley, K., et. al., Nature, 372, (1994), pp. 652-654.
101. M. Chown, "Astronomers claim dark matter breakthrough," NewScientist.com, Oct. 3,

(2003), http://www.newscientist.com/ article/dn4214-astronomers-claim-dark-matter-breakthrough.html.
102. C. Boehm, D. Hooper, J. Silk, M. Casse, J. Paul, "MeV dark matter: Has it been detected," Phys. Rev. Lett., Vol. 92, (2004), p. 101301.
103. T. Van Flandern, "The Speed of Gravity—What the Experiments Say," Physics Letters A, 250 (1998), pp. 1-11.
104. R. Cowen, Science News, May 9, (1998), p. 292.
105. M. Chown, New Scientist, May 10, (1997), p. 21.
106. B. Schwarzschild, Physics Today, Vol. 51, No. 10, October, (1998), pp. 19-21.
107. G. Taubes, "Pattern emerges in cosmic ray mystery," Science, News Series, Vol. 262, No. 5140, (Dec. 10, 1993), p. 1649.
108. D. J. Bird, et al., "Evidence for correlated changes in the spectrum and composition of cosmic rays at extremely high energies," Physical Review Letters, Vol. 71, No. 21, (1993), pp. 3401-3404.
109. W. McC. Siebert, *Circuits, Signals, and Systems*, The MIT Press, Cambridge, Massachusetts, (1986), pp. 597-603.
110. S. D. Landy, Scientific American, June, (1999), pp. 38-45.
111. G. R. Fowles, *Analytical Mechanics*, Third Edition, Holt, Rinehart, and Winston, New York, (1977), pp. 57-60.
112. C. Willott, "A monster in the early Universe," Nature, Vol. 474, (2011), pp.583-584.
113. D.J. Mortlock,et al., "A luminous quasar at a redshift of z=7.085," Nature, Vol. 474, (2011), pp. 616-619.
114. G. Musser, Scientific American, Vol. 278, No. 3, March, (1998), p. 18.
115. P. de Bernardis, et al., A flat universe from high-resolution maps of the cosmic microwave background radiation, Nature, Vol. 404, (2000), p. 955; http://cmb.phys.cwru.edu/boomerang.
116. K. Sawyer, "Supernova observations bolster dark energy theory," April 3, (2001), washingtonpost.com.
117. A. G. Riess, et. al. "The farthest known supernova: support for an accelerating universe and a glimpse of the epoch of deceleration," Astrophysical Journal, Vol. 560, (2001), pp. 49-71.
118. B. P. Abbott, R Abbott, R. Adhikari, P. Ajith, B. Allen, G. Allen, R. S. Amin, S. B. Anderson, W. G. Anderson, M. A. Arain; et al., "LIGO: the Laser Interferometer Gravitational-Wave Observatory," Rep. Prog. Phys. 72 (2009) 076901 (25pp).
119. P. Shawhan, "Gravitational-wave astronomy: observational results and their impact," Class. Quantum Grav., Vol. 27 (2010) 084017 (14 pp).
120. J. H. Phillips, *Guide to the Sun*, Cambridge University Press, Cambridge, Great Britain, (1992), pp. 58-67.
121. A. Davidsen, et al., "Test of the decaying dark matter hypothesis using the Hopkins ultraviolet telescope," Nature, 351, (1991), pp. 128-130.
122. W. Milan, "Shall the WIMPs Inherit the Universe," SPACE.com, 28, February, 2000, http://space.com/scienceastronomy/ generalscience/dark_matter_000228.html.
123. R. Abusaidi, et al., "Exclusion limits on the WIMP-nucleon cross section from the cryogenic dark matter search," Physical Review Letters, Vol. 84, No. 25, 19, June, (2000), pp. 5699-5703.

124. R. N. Bracewell, *The Fourier Transform and Its Applications*, McGraw-Hill Book Company, New York, (1978), pp. 252-253.
125. W. McC. Siebert, *Circuits, Signals, and Systems*, The MIT Press, Cambridge, Massachusetts, (1986), p. 415.
126. B. R. Oppenheimer, N. C. Hambly, A. P. Digby, S. T. Hodgkin, and D. Saumon, "Direct detection of galactic halo dark matter," Science, Vol. 292, 27, April, (2000), pp. 698-702.
127. M. Zaldarriaga, "Background comes to the fore," Nature, Vol. 420, No. 6917, (2002), pp. 747-748.
128. E. M. Leitch, J. M. Kovac, C. Pryke, J. E. Carlstrom, N. W. Halverson, W. L. Holzapfel, M. Dragovan, B. Reddall, E. S. Sandberg, "Measurement of the polarization with the Degree Angular Scale Interferometer," Nature, Vol. 420, No. 6917, (2002), pp. 763-771.
129. J. M. Kovac, E. M. Leitch, C. Pryke, J. E. Carlstrom, N. W. Halverson, W. L. Holzapfel, "Detection of polarization in the cosmic microwave background using DASI," Nature, Vol. 420, No. 6917, (2002), pp. 772-787.
130. G. Hinshaw, *et al*., "Nine-year Wilkinson Microwave Anisotropy Probe (WMAP) observations: Cosmological parameters results", The Astrophysical Journal Supplement Series, Vol. 208. No.19, (2013), pp. 1-25.
131. H. C. Chiang, P. A. R. Ade, D. Barkats, J. O. Battle, E. M. Bierman, J. J. Bock, C. D. Dowell, L. Duband, E. F. Hivon, W. L. Holzapfel, V. V. Hristov, W. C. Jones, B. G. Keating, J. M. Kovac, C. L. Kuo, A. E. Lange, E. M. Leitch, P. V. Mason, T. Matsumura, H. T. Nguyen, N. Ponthieu, C. Pryke, S. Richter, G. Rocha, C. Sheehy, Y. D. Takahashi, J. E. Tolan, K. W. Yoon, "Measurement of cosmic microwave background polarization power spectra from two years of BICEP data", The Astrophysical Journal, Vol. 711, pp. 1123-1140.
132. Bicep2 Collaboration – P. A. R. Ade, R. W. Aikin, D. Barkats, S. J. Benton, C. A. Bischoff, J. J. Bock, J. A. Brevik, I. Buder, E. Bullock, C. D. Dowell, L. Duband, J. P. Filippini, S. Fliescher, S. R. Golwala, M. Halpern, M. Hasselfield, S. R. Hildebrandt, G. C. Hilton, V. V. Hristov, K. D. Irwin, K. S. Karkare, J. P. Kaufman, B. G. Keating, S. A. Kernasovskiy, J. M. Kovac, C. L. Kuo, E. M. Leitch, M. Lueker, P. Mason, C. B. Netterfield, H. T. Nguyen, R. O'Brient, R. W. Ogburn IV, A. Orlando, C. Pryke, C. D. Reintsema, S. Richter, R. Schwarz, C. D. Sheehy, Z. K. Staniszewski, R. V. Sudiwala, G. P. Teply, J. E. Tolan, A. D. Turner, A. G. Vieregg, C. L. Wong, K. W. Yoon, "Bicep2 I: Detection of B-mode polarization at degree angular scales, http://arxiv.org/pdf/1403.3985.pdf.